Inorg. Chem. **2008**, *47*, 9779−9796

Site Selectivity in the Protonation of a Phosphinito Bridged $Pt^{I}-Pt^{I}$ Complex: a Combined NMR and Density-Functional Theory Mechanistic Study†

Mario Latronico,‡ Flavia Polini,‡ Vito Gallo,‡ Piero Mastrorilli,*,‡ Beatrice Calmuschi-Cula,§ Ulli Englert,§ Nazzareno Re,|| Timo Repo,⊥ and Minna Räisänen⊥

Dipartimento di Ingegneria delle Acque e di Chimica del Politecnico di Bari, Via Orabona 4, I-70125 Bari, Italy, Institut für Anorganische Chemie der RWTH, Landoltweg 1, D-52074 Aachen, Germany, Dipartimento di Scienze del Farmaco, Università "G. d'Annunzio", Via dei Vestini 31, 06100 Chieti, Italy, and Laboratory of Inorganic Chemistry, Department of Chemistry, University of Helsinki, P.O. Box 55, FIN-00014 Helsinki, Finland

Received March 20, 2008

The protonation of the dinuclear phosphinito bridged complex $[(PHCy_2)Pt(\mu\text{-}PCy_2)\{\kappa^2P,O\text{-}\mu\text{-}P(O)Cy_2\}Pt(PHCy_2)]$ (*Pt*−*Pt*) (**1**) by Brønsted acids affords hydrido bridged Pt−Pt species the structure of which depends on the nature and on the amount of the acid used. The addition of 1 equiv of HX (X = Cl, Br, I) gives products of formal protonation of the Pt−Pt bond of formula *syn*-$[(PHCy_2)(X)Pt(\mu\text{-}PCy_2)(\mu\text{-}H)Pt(PHCy_2)\{\kappa P\text{-}P(O)Cy_2\}]$ (*Pt*−*Pt*) (**5**, X = Cl; **6**, X = Br; **8**, X = I), containing a Pt−X bond and a dangling κP-$P(O)Cy_2$ ligand. Uptake of a second equivalent of HX results in the protonation of the $P(O)Cy_2$ ligand with formation of the complexes $[(PHCy_2)(X)Pt(\mu\text{-}PCy_2)(\mu\text{-}H)Pt(PHCy_2)\{\kappa P\text{-}P(OH)Cy_2\}]X$ (*Pt*−*Pt*) (**3**, X = Cl; **4**, X = Br; **9**, X = I). Each step of protonation is reversible, thus reactions of **3**, **4**, with NaOH give, first, the corresponding neutral complexes **5**, **6**, and then the parent compound **1**. While the complexes **3** and **4** are indefinitely stable, the iodine analogue **9** transforms into *anti*-$[(PHCy_2)(I)Pt(\mu\text{-}PCy_2)(\mu\text{-}H)Pt(PHCy_2)(I)]$ (*Pt*−*Pt*) (**7**) deriving from substitution of an iodo group for the $P(OH)Cy_2$ ligand. Complexes **3** and **4** are isomorphous crystallizing in the triclinic space group $P\bar{1}$ and show an intramolecular hydrogen bond and an interaction between the halide counteranion and the POH hydrogen. The occurrence of such an interaction also in solution was ascertained for **3** by ^{35}Cl NMR. Multinuclear NMR spectroscopy (including $^{31}P-^{1}H$ HOESY) and density-functional theory calculations indicate that the mechanism of the reaction starts with a prior protonation of the oxygen with formation of an intermediate (**12**) endowed with a six membered $Pt^1-X\cdots H-O-P-Pt^2$ ring that evolves into thermodynamically stable products featuring the hydride ligand bridging the Pt atoms. Energy profiles calculated for the various steps of the reaction between **1** and HCl showed very low barriers for the proton transfer and the subsequent rearrangement to **12**, while a barrier of 29 kcal mol^{-1} was found for the transformation of **12** into **5**.

Introduction

The site selectivity in proton transfer reactions has attracted considerable interest in the recent literature.[1] In this contribution, we report on the reactivity of a dialkylphosphinito bridged diplatinum complex toward several Brønsted acids and on the mechanistic study of the consequent protonations. Dialkylphosphinito bridged homodinuclear complexes are interesting compounds as the differentiation of the two metal centers brought about by the combination of a soft donor (P) and a hard ligand (O) may result in peculiar reactivity.

In this regard we started a project aimed to investigate the reactivity of $[(PHCy_2)Pt(\mu\text{-}PCy_2)\{\kappa^2P,O\text{-}\mu\text{-}P(O)Cy_2\}\text{-}Pt(PHCy_2)]$ (*Pt*−*Pt*) (**1**),[2] the first unsymmetrical phosphinito bridged Pt complex, toward several types of reactants. We have recently reported that **1** reacts with nucleophiles such

† Dedicated to Prof. Cosimo Francesco Nobile on occasion of his 70th birthday.

* To whom correspondence should be addressed. E-mail: p.mastrorilli@poliba.it.

‡ Dipartimento di Ingegneria delle Acque e di Chimica del Politecnico di Bari.

§ Institut für Anorganische Chemie der RWTH.

⊥ University of Helsinki.

|| Università "G. d'Annunzio".

(1) Evrard, D.; Clément, S.; Lucas, D.; Hanquet, B.; Knorr, M.; Strohmann, C.; Decken, A.; Mugnier, Y.; Harvey, P. D. *Inorg. Chem.* **2006**, *45*, 1305–1315; and references cited therein.

(2) Gallo, V.; Latronico, M.; Mastrorilli, P.; Nobile, C. F.; Suranna, G. P.; Ciccarella, G.; Englert, U. *Eur. J. Inorg. Chem.* **2005**, 4607–4616.

10.1021/ic800508t CCC: $40.75 © 2008 American Chemical Society
Published on Web 10/01/2008

as $PHCy_2$, PCy_3, $P(S)HCy_2$, and $P(O)HCy_2$ giving substitution or addition products depending on the nucleophile[3] (Scheme 1). It has been underlined that the oxygen end of the μ-phosphinito ligand can exercise control over the sites of substitution, as demonstrated in the cases of dinuclear Ru complexes.[4] In our case such a control resulted in an attack of the incoming nucleophiles [$PHCy_2$, PCy_3, $P(S)HCy_2$] on **1** exclusively to the O-bound Pt atom, which behaves as the most electrophilic center of the molecule. However, the reaction of **1** with $P(O)HCy_2$ led selectively to the hydrido bridged dinuclear complex *syn*-[$(PHCy_2)\{\kappa P\text{-}P(O)Cy_2\}Pt(\mu\text{-}PCy_2)(\mu\text{-}H)Pt(PHCy_2)\{\kappa P\text{-}P(O)Cy_2\}$] (*Pt*−*Pt*) (**2**) which represents the product of formal protonation of the Pt^I-Pt^I bond by a relatively weak acid [the $P(OH)Cy_2$ tautomeric form of the dicyclohexylphosphane oxide]. These findings indicated that **1** behaves as an amphiphilic molecule, capable of reacting with both nucleophiles and electrophiles, and such view was confirmed by a thorough density-functional theory (DFT) study which showed that **1** possesses a strongly electrophilic center (the O-bound Pt^1) and four nucleophilic centers (in increasing order of nucleophilicity: P^4, Pt^2, P^2, and O) as inferred from the Mulliken gross atomic charges outlined in Figure 1.[3]

The protonation of the Pt^I-Pt^I bond that occurred when **1** was reacted with $P(O)HCy_2$ seems to be in contrast with the DFT predictions, since the order of nucleophilicity indicates the O (which remains deprotonated) as the most basic site of **1**. This seeming discrepancy prompted us to study the protonation of **1** by several Brønsted acids and to gain insights into the mechanism of proton transfer from the acid to the final product.

The elucidation of factors governing the site selectivity in reactions between polynuclear transition metal complexes and electrophilic reagents is a matter of long standing interest, especially when the complexes are phosphanido bridged dinuclear species featuring a metal−metal bonds.[5] As far as protonation reactions are concerned, a wealth of synthetic and mechanistic studies dealing with the reaction of H^+ with transition metal hydrides showed the formation of "unconventional" intramolecular and intermolecular hydrogen bonds involving the hydride ligand as a proton acceptor.[6]

The first report on H^+ attack on dinuclear metal complexes dates back to 1962 and deals with the formation of a series of homo and heterodinuclear carbonyl cyclopentadienyl clusters in which the two metals are linked by a metal−metal bond and are bridged by a hydride ligand.[7] The formation of a bridging hydride by protonation of the metal−metal bond is the rule for complexes not bearing bridging phosphanido groups as reported in the cases of $[Et_4N][Cr_2(CO)_{10}]$,[8] $[CpM(\mu\text{-}CO)(CO)]_2$ (M = Fe[9] or Ru[10]), $[\mu\text{-}(SCH_3)Fe(CO)_2L]_2$ [$L = P(CH_3)_{3-x}(C_6H_5)_x$],[11] $(\mu\text{-}CO)[CpRh(CO)]_2$,[12] $(\mu\text{-}CH_2)[CpRh(CO)]_2$,[13] $[Cp_2Re_2(CO)_5]$,[14] $[Rh_2Cl_2(\mu\text{-}CO)(\mu\text{-dppm})]$,[15] and $[Cp_2Rh_2(\mu\text{-}CO)(\mu\text{-dppm})]$.[16]

On the contrary, a variety of protonation products can be obtained when the two metals are bridged by a phosphanido group. Bridging hydrides are formed by protonation of $[Fe_2(\mu\text{-}A)(\mu\text{-}A')(CO)_4L_2]$ [$A = A' = PPh_2$, PMe_2; $A = SPh$, $A' = PPh_2$; $L = P(CH_3)_{3-x}(C_6H_5)_x$],[17] $[NEt_4][(CO)_4Mn(\mu\text{-}PTol_2)Mo(CO)_2Cp]$ (*Mn*−*Mo*),[18] $[Cp_2Co_2(\mu\text{-}PR_2)_2]$ (PR_2 = PMe_2, PPh_2, PEt_2, PMePh, $^1/_2Ph_2P(CH_2)_nPPh_2$, $n = 2$ or 3),[19] $[CpMo(\mu\text{-}PPh_2)CO)]_2$,[20] $[m(\mu\text{-}PPh_2)Pt(PPh_3)_2]$ [m = $W(CO)_2Cp$, $Mn(CO)_4$, $Co(CO)_3$],[21] $[Cp^*Rh(\mu\text{-}PMe_2)]_2$,[22] or $[Cp(CO)_2Mo(\mu\text{-}PPh_2)Pt(CO)(PPh_3)]$.[23] Interestingly, the related complexes $[Cp(CO)_2W(\mu\text{-}PPh_2)Pt(CO)(PPh_3)]$ and $[Cp(CO)_2W(\mu\text{-}PCy_2)Pt(CO)(PCy_2H)]$ give, the first protonation directly at the tungsten to give $[Cp(CO)_2(H)W(\mu\text{-}PPh_2)Pt(CO)(PPh_3)]^+$,[23] the second both isomeric hydrides $[Cp(CO)_2W(\mu\text{-}PCy_2)(\mu\text{-}H)Pt(CO)(PCy_2H)]^+$ and $[Cp(H)(CO)_2W(\mu\text{-}PCy_2)Pt(CO)\ (PCy_2H)]^+$ of which the former is the major product.[24]

The protonation of the dianion $[(CO)_3Fe(\mu\text{-}PPh_2)_2Fe(CO)_3]^{2-}$ (*Fe*−*Fe*) affords, as main product, $[(CO)_2HFe(\mu\text{-}PPh_2)_2(\mu\text{-}CO)Fe(CO)_3]^-$ in which the hydride is terminally bonded and the metal−metal bond is broken.[25] In the case of the related anions $[(CO)_3Fe(\mu\text{-}PPh_2)(\mu\text{-}CO)_2Fe(CO)_2(PHPh_2)]^-$ (*Fe*−*Fe*) or $[(CO)_4W(\mu\text{-}PPh_2)_2Rh(CO)(PPh_3)]^-$

(3) Gallo, V.; Latronico, M.; Mastrorilli, P.; Nobile, C. F.; Polini, F.; Re, N.; Englert, U. *Inorg. Chem.* **2008**, *47*, 4785–4795.
(4) Fogg, D. E.; Carty, A. J. *Polyhedron* **1988**, *7*, 2285–2295.
(5) (a) Alvarez, M. A.; Garcia, M. E.; Martinez, M. E.; Ramos, A.; Ruiz, M. A.; Saez, D.; Vaissermann, J. *Inorg. Chem.* **2006**, *45*, 6965–6978. (b) Archambault, C.; Bender, R.; Braunstein, P.; Dusausoy, Y. *Dalton Trans.* **2002**, 4084–4090.
(6) (a) Belkova, N. V.; Shubina, E. S.; Epstein, L. M. *Acc. Chem. Res.* **2005**, *38*, 624–631; and refs cited therein. (b) Bakhmutov, V. I. *Eur. J. Inorg. Chem.* **2005**, 245–255; and refs cited therein. (c) Belkova, N. V.; Collange, E.; Dub, P.; Epstein, L. M.; Lemenovskii, D. A.; Lledos, A.; Maresca, O.; Maseras, F.; Poli, R.; Revin, P. O.; Shubina, E. S.; Vorontsov, E. V. *Chem.*−*Eur. J.* **2005**, *11*, 873–888. (d) Belkova, N. V.; Revin, P. O.; Besora, M.; Baya, M.; Epstein, L. M.; Lledos, A.; Poli, R.; Shubina, E. S.; Vorontsov, E. V. *Eur. J. Inorg. Chem.* **2006**, 2192–2209. (e) Algarra, A. G.; Basallote, M. G.; Fernandez-Trujillo, M. J.; Llusar, R.; Safont, V. S.; Vicent, C. *Inorg. Chem.* **2006**, *45*, 5774–5784. (f) Algarra, A. G.; Basallote, M. G.; Feliz, M.; Fernandez-Trujillo, M. J.; Llusar, R.; Safont, V. S. *Chem.*−*Eur. J.* **2006**, *12*, 1413–1426. (g) Dub, P. A.; Baya, M.; Houghton, J.; Belkova, N. V.; Daran, J.-C.; Poli, R.; Epstein, L. M.; Shubina, E. S. *Eur. J. Inorg. Chem.* **2007**, 2813–2826.
(7) Davison, A.; McFarlane, W.; Pratt, L.; Wilkinson, G. *J. Chem. Soc. A* **1962**, 3653–3666.
(8) Hayter, R. G. *J. Am. Chem. Soc.* **1966**, *88*, 4376–4382.
(9) Symon, D. A.; Waddington, T. C. *J. Chem. Soc. A* **1971**, 953–957.
(10) Harris, D. C.; Gray, H. B. *Inorg. Chem.* **1975**, *14*, 1215–1217.
(11) Fauvel, K.; Mathieu, R.; Poilblanc, R. *Inorg. Chem.* **1976**, *15*, 976–978.
(12) Herrmann, W. A.; Plank, J.; Riedel, D. *J. Organomet. Chem.* **1980**, *190*, C47–C50.
(13) Herrmann, W. A.; Plank, J.; Riedel, D.; Ziegler, M. L.; Weidenhammer, K.; Guggolz, E.; Balbach, B. *J. Am. Chem. Soc.* **1981**, *103*, 63–75.
(14) Lewis, L. N.; Caulton, K. G. *Inorg. Chem.* **1981**, *20*, 1139–1142.
(15) Sutherland, B. R.; Cowie, M. *Inorg. Chem.* **1984**, *23*, 1290–1297.
(16) Lo Schiavo, S.; Bruno, G.; Nicolò, F.; Piraino, P.; Faraone, F. *Organometallics* **1985**, *4*, 2091–2096.
(17) Arabi, M. S.; Mathieu, R.; Poilblanc, R. *J. Organomet. Chem.* **1979**, *177*, 199–209.
(18) Casey, C. P.; Bullock, R. M. *Organometallics* **1984**, *3*, 1100–1104.
(19) (a) Chen, L.; Kountz, D. J.; Meek, D. W. *Organometallics* **1985**, *4*, 598–601. (b) Werner, H.; Hofmann, W.; Zolk, R.; Dahl, L. F.; Kocal, J.; Kühn, A. *J. Organomet. Chem.* **1985**, *289*, 173–188.
(20) Adatia, T.; McPartlin, M.; Mays, M. J.; Morris, M. J.; Raithby, P. R. *J. Chem. Soc., Dalton Trans.* **1989**, 1555–1564.
(21) Braunstein, P.; deJesùs, E.; Tiripicchio, A.; Uguzzoli, F. *Inorg. Chem.* **1992**, *31*, 411–418.
(22) Klingert, B.; Werner, H. *J. Organomet. Chem.* **1983**, *252*, C47–C52.
(23) Powell, J.; Sawyer, J. F.; Smith, S. J. *J. Chem. Soc., Chem. Commun.* **1985**, 1312–1313.
(24) Blum, T.; Braunstein, P. *Organometallics* **1989**, *8*, 2497–2503.
(25) Collman, J. P.; Rothrock, R. K.; Finke, R. G.; Moore, E. J.; Rose-Munch, F. *Inorg. Chem.* **1982**, *21*, 146–156.

Scheme 1. Reaction of **1** with Nucleophiles

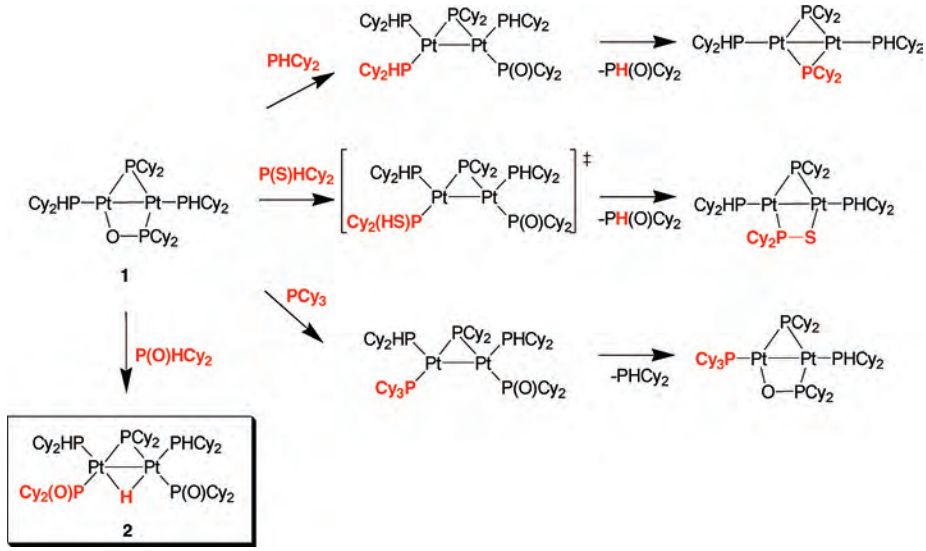

($W-Rh$) the attack of H^+ results in the terminal hydride species $[(CO)_3HFe(\mu\text{-}PPh_2)Fe(PHPh_2)(CO)_3]$ ($Fe-Fe$)[26] and $[(CO)_4W(\mu\text{-}PPh_2)_2Rh(CO)(H)(PPh_3)]$ ($W-Rh$)[27] without rupture of the metal−metal bond. In the case of $[(CO)_4W(\mu\text{-}PPh_2)_2Os(CHO)(CO)_2L]^-$ (L = $PMePh_2$, PMe_3) one of the bridging phosphanides is protonated to the corresponding phosphane, giving the neutral complex $[(CO)_4W(\mu\text{-}PPh_2)Os(PHPh_2)(CHO)(CO)_2L]$ (L = $PMePh_2$, PMe_3).[28] The disruption of the dinuclear unit is the result of the protonation of bridging phosphanides in $[(CO)_4M(\mu\text{-}PPh_2)M(CO)_4(PHPh_2)]^-$ (M = W or Mo), which gives a mixture of *cis*-$[M(CO)_4(PHPh_2)_2]$ and $[M(CO)_5(PHPh_2)]$[29] and in $[(PHCy_2)Pd(\mu\text{-}PCy_2)(\mu\text{-}\eta^3\text{-}C_3H_5)Pd(PHCy_2)]$ which gives, upon reaction with PhSH or PhSeH, the mononuclear complexes *trans*-$[Pd(EPh)_2(PHCy_2)_2]$ (E = S or Se, respectively).[30] It is noteworthy that the dimer $[(PH^tBu_2)Pd(\mu\text{-}P^tBu_2)_2Pd(PH^tBu_2)]$ readily protonates to give the unusual cationic Pd^I complex $[(PH^tBu_2)Pd(\mu\text{-}P^tBu_2)(\mu\text{-}PH^tBu_2)Pd(PH^tBu_2)]$ containing a Pd−H−P bridging unit.[31] The related agostic type phosphane bridged complexes $[Mo_2Cp_2(\mu\text{-}PR_2)(\mu\text{-}\kappa^2\text{-}HPR_2)(CO)_2]^+$ (R = Cy, Et) were recently reported by Ruiz and co-workers.[5a]

The only previous examples dealing with protonation of dinuclear phosphanido bridged diplatinum complexes with strong acids have been reported by Leoni et al. and by Braunstein et al. It has been found that addition of triflic acid to $[Pt(\mu\text{-}P^tBu_2)(H)(P^tBu_2H)]_2$ results in the formation of $[(PH^tBu_2)_2Pt(\mu\text{-}H)(\mu\text{-}P^tBu_2)Pt(H)(PH^tBu_2)]^+$,[32] whereas the Pt^I dimer $[(PH^tBu_2)Pt(\mu\text{-}P^tBu_2)]_2$ gives the terminal hydrido complex $[(PH^tBu_2)Pt(\mu\text{-}P^tBu_2)_2Pt(H)(PH^tBu_2)]^+$ by attack of H^+ on one of the Pt atoms.[33] In the case of $[(PH^tBu_2)Pt(\mu\text{-}P^tBu_2)_2Pt(CO)]$, the kinetic product $[(PH^tBu_2)Pt(\mu\text{-}P^tBu_2)_2Pt(H)(CO)]^+$ is converted by an external base into the thermodynamically favored form $[(PH^tBu_2)(H)Pt(\mu\text{-}P^tBu_2)_2Pt(CO)]^+$.[33] The "mixed bridge" complex $[(PPh_3)Pt(\mu\text{-}PPh_2)(\mu\text{-}o\text{-}C_6H_4PPh_2)Pt(PPh_3)]$ reacts with 1 equiv of acid giving the cation $[(PPh_3)Pt(\mu\text{-}H)(\mu\text{-}PPh_2)(\mu\text{-}o\text{-}C_6H_4PPh_2)Pt(PPh_3)]^+$ or with 2 equiv of acid to give $[(PPh_3)(solvent)Pt(\mu\text{-}H)(\mu\text{-}PPh_2)Pt(PPh_3)_2]^{2+}$.[5b] Finally, the protonation of $[Pt(\mu\text{-}P^tBu_2)(\eta^2\text{-}C_2H_4)]_2$ affords $[Pt_2(\mu\text{-}P^tBu_2)(\mu\text{-}PH^tBu_2)(\eta^2\text{-}C_2H_4)_2]^+$ with a P−H−M agostic proton in rapid exchange with those of the adjacent ethylene molecule.[34]

In the light of the rich chemistry summarized above, complex **1**, featuring both a bridging phosphanido and dialkylphosphinito groups, represents an ideal benchmark for a study of the site selectivity in the electrophilic attack on a polynuclear complex endowed with metal−metal bonds. In fact, besides the previously discussed protonation sites (i.e., the metal atoms, the metal−metal bond, and the metal−phosphorus bond) **1** is endowed with a further target site represented by the phosphinito oxygen.

Results and Discussion

Synthesis of Cationic Complexes by Reactions with HX (X = Cl, Br). The reactions between **1** and excess HCl (gaseous or aqueous) or HBr (gaseous or aqueous) in *n*-hexane led to the new hydrido bridged complexes **3** and **4** in isolated yields higher than 90% (Scheme 2). As the products **3** and **4** share the same spectroscopic features, we will only discuss those of **3** in the following section.

The $^{31}P\{^1H\}$ NMR spectrum of **3** (Figure 2) resembles that of the parent complex **1**, consisting of four mutually

(26) Yu, Y.-F.; Gallucci, J.; Wojcicki, A. *J. Am. Chem. Soc.* **1983**, *105*, 4826–4828.
(27) Geoffroy, G. L.; Rosenberg, S.; Shulman, P. M.; Whittle, R. R. *J. Am. Chem. Soc.* **1984**, *106*, 1519–1521.
(28) Rosenberg, S.; Whittle, R. R.; Geoffroy, G. L. *J. Am. Chem. Soc.* **1984**, *106*, 5934–5940.
(29) Shyu, S.-G.; Wojcicki, A. *Organometallics* **1984**, *3*, 809–812.
(30) (a) Pasquali, M.; Marchetti, F.; Leoni, P.; Beringhelli, T.; D'Alfonso, G. *Gazz. Chim. Ital.* **1993**, *11*, 659–664. (b) Sommovigo, M.; Pasquali, M.; Marchetti, F.; Leoni, P.; Beringhelli, T. *Inorg. Chem* **1994**, *33*, 2651–2656.
(31) (a) Albinati, A.; Lianza, F.; Pasquali, M.; Sommovigo, M.; Leoni, P.; Pregosin, P. S.; Ruegger, H. *Inorg. Chem.* **1991**, *30*, 4690–4692. (b) Leoni, P.; Pasquali, M.; Sommovigo, M.; Laschi, F.; Zanello, P.; Albinati, A.; Lianza, F.; Pregosin, P. S.; Ruegger, H. *Organometallics* **1993**, *12*, 1702–1713.
(32) Leoni, P.; Manetti, S.; Pasquali, M. *Inorg. Chem.* **1995**, *34*, 749–752.
(33) Leoni, P.; Pasquali, M.; Cittadini, V.; Fortunelli, A.; Selmi, M. *Inorg. Chem.* **1999**, *38*, 5257–5265.
(34) Leoni, P.; Marchetti, F.; Marchetti, L.; Passarelli, V. *Chem. Commun.* **2004**, 2346–2347.

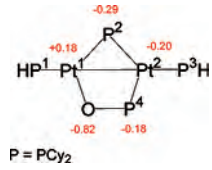

Figure 1. Mulliken gross atomic charges for the Pt_2P_2O core of complex **1**.

Scheme 2. Protonation of **1** with HCl or HBr

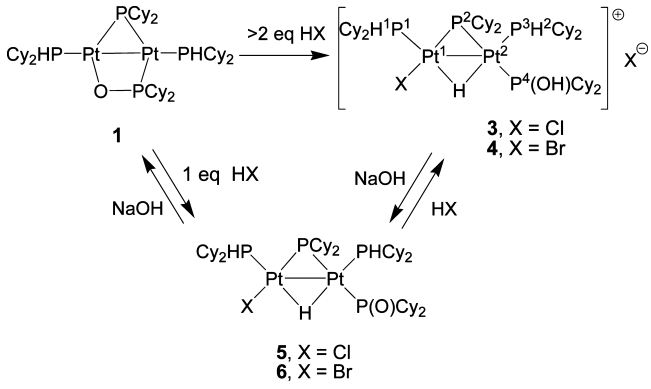

coupled signals (all flanked by ^{195}Pt satellites) at δ 155.3 (P^2), δ 118.8 (P^4), δ 10.8 (P^1), and δ 5.2 (P^3).

The ^{195}Pt signals were found at δ −5379 (Pt^1) and δ −5621 (Pt^2) (Figure 3). Differently from the parent compound **1**, which did not show any ^{195}Pt−^{195}Pt coupling, a $J_{Pt,Pt}$ of 845 Hz was directly extracted from the ^{195}Pt{^{1}H} NMR spectrum.

The presence of the bridging hydride is unequivocally demonstrated by the ^{1}H NMR spectrum showing a multiplet centered at δ −5.61 flanked by three sets of ^{195}Pt satellites, while a broad signal at δ 10.8[35] is diagnostic for the presence of the PO*H* moiety. The attribution of the hydride NMR features was made using the data directly extractable from the ^{1}H−^{195}Pt HMQC spectrum of **3** (Figure 4). The hydrogens directly bound to P fall at δ 4.58 (P^1H) and δ 5.12 (P^3H) and were attributed by the ^{1}H−^{31}P HMQC spectrum (Supporting Information, Figure S1). Of these signals, that at δ 4.58 is sharper ($\Delta\nu_{1/2}$ are 46 Hz for P^1H and 92 Hz for P^3H) and shows a significantly higher coupling constant with the vicinal Pt atom ($^2J_{H(1),Pt(1)}$ = 158 Hz vs $^2J_{H(2),Pt(2)}$ = 29 Hz). Similar features were found for the complexes described hereafter having the same scaffold (compounds **4**, **5**, **6**, **8**, **9**, **11**, **15**, **16**, **19**).

The broadness of the signals attributed to P^3 and P^4 might be explainable in terms of hindered rotation about the P−Pt bonds because of the steric hindrance brought about by the cyclohexyl groups.[36] The dynamic behavior alleged for **3** can be held responsible also for the broadness of the multiplet

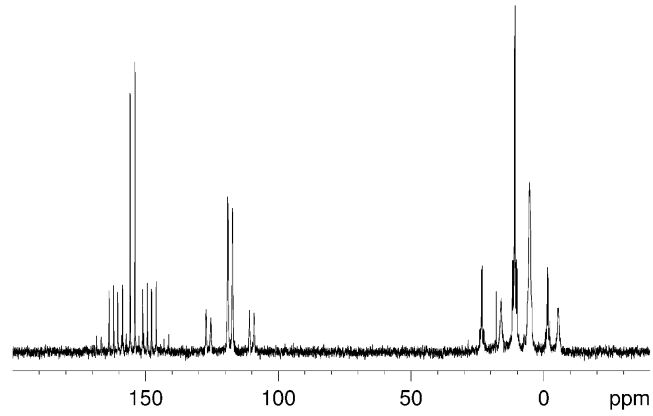

Figure 2. ^{31}P{^{1}H} NMR spectrum of **3** (CD_2Cl_2, 295 K).

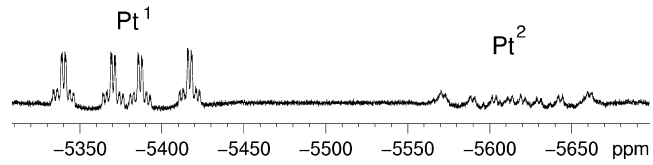

Figure 3. ^{195}Pt{^{1}H} NMR spectrum of **3** (CD_2Cl_2, 295 K).

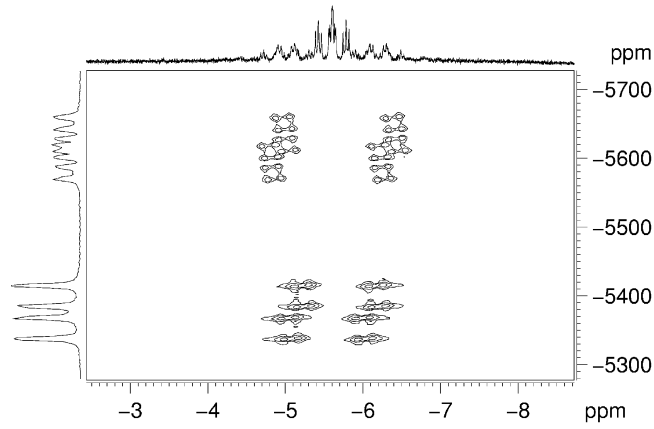

Figure 4. ^{1}H−^{195}Pt HMQC spectrum of **3** (hydride region, CD_2Cl_2, 295 K).

attributed to Pt^2 compared to that of Pt^1 (Figure 3). A possible interaction between the cationic complex and the chloride counteranion should be also taken into account. We have previously demonstrated that the chloride counteranion strongly interacts with the H−P of cationic Pt^{II} complexes such as $[Pt(PHCy_2)_3Cl]Cl$[36] and $[Pt(PHCy_2)_2(\kappa^2S,S'\text{-}PS_2Cy_2)]Cl$[37] and that ^{35}Cl NMR spectroscopy is a useful tool to detect the presence of "free" chlorides in solution.[38] Interestingly, the ^{35}Cl NMR spectrum of **3** in CD_2Cl_2 gave no signal even in the presence of methanol, thus suggesting that complex **3** behaves as an intimate ion couple not only in solvents with low dielectric constant (CD_2Cl_2) but also in the presence of a classic hydrogen bond breaker such as methanol. Given that PH···Cl^- interactions are easily

(35) The chemical shift of this signal was found sensitive to the presence of traces of moisture in the deuterated solvent.

(36) Broadening of ^{31}P NMR signals due to hindered rotation occurs in the related phosphanido bridged complexes $[(Cy_2PH)(Cl)Pt(\mu\text{-}PCy_2)Pt(Cy_2PH)_2]$ (Pt-Pt) [(a) Mastrorilli, P.; Nobile, C. F.; Fanizzi, F. P.; Latronico, M.; Hu, C.; Englert, U. *Eur. J. Inorg. Chem.* **2002**, 1210–1218.] and *syn*-$[(Cy_2PH)(\kappa P\text{-}POCy_2)Pt(\mu\text{-}PCy_2)(\mu\text{-}H)Pt(Cy_2PH)(\kappa P\text{-}POCy_2)]$ (Pt-Pt) [(b) Ref 3]. The hindered rotation about the P-Pt bonds of dicyclohexylphosphane derivatives is discussed in (c) Mastrorilli, P.; Nobile, C. F.; Latronico, M.; Gallo, V.; Englert, U.; Fanizzi, F. P.; Sciacovelli, O. *Inorg. Chem.* **2005**, *44*, 9097–9104.

(37) Gallo, V.; Latronico, M.; Mastrorilli, P.; Nobile, C. F.; Ciccarella, G.; Englert, U. *Eur. J. Inorg. Chem.,* **2006**, 2634–2641.

(38) NMR signals of quadrupolar nuclei such as ^{35}Cl are strongly affected by the symmetry of the surrounding electronic cloud. Thus, when a chloride counteranion of a metal complex forms an intimate ion couple, the ^{35}Cl NMR signal usually does not emerge from the baseline unless a solvent able to disrupt the ion couple and to form a nearly symmetric solvation sphere is added.

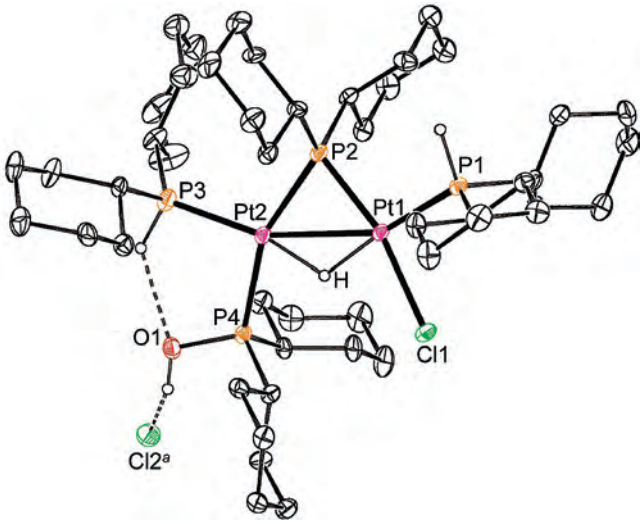

Figure 5. PLATON drawing of **3**·$3CH_2Cl_2$; displacement ellipsoids are scaled to 30% probability; the solvent molecules and H atoms bonded to carbon have been omitted for clarity. Interatomic distances (Å) and angles (deg) [values for **4**·$3CH_2Cl_2$ in square brackets]: Pt1−P2 2.243(2) [2.2173(17)]; Pt1−P1 2.280(3) [2.2509(17)]; Pt1−Cl1 2.412(2) [Pt1−Br1 2.4949(8)]; Pt1−H 1.71 [1.70]; Pt2−P3 2.306(3) [2.2764(18)]; Pt2−P4 2.328(3) [2.2915(18)]; Pt2−P2 2.337(3) [2.3050(18)]; Pt2−H 1.69 [1.64]; Pt1−Pt2 2.8778(15) [2.8379(4)]; P2−Pt1−P1 101.63(10) [101.71(6)]; P2−Pt1−Cl1 166.37(9) [P2−Pt1−Br1 165.49(5)]; P1−Pt1−Cl1 91.48(9) [P1−Pt1−Br1 92.09(5)]; P2−Pt1−Pt2 52.56(7) [52.52(4)]; P1−Pt1−Pt2 153.98(6) [154.07(4)]; Cl1−Pt1−Pt2 114.09(7) [Br1−Pt1−Pt2 113.39(2)]; P2−Pt1−H 84.4 [83.8]; P1−Pt1−H 173.0 [173.9]; Cl1−Pt1−H 82.3 [Br1−Pt1−H 82.2]; P3−Pt2−P4 93.23(9) [92.94(7)]; P3−Pt2−P2 108.01(9) [107.69(7)]; P4−Pt2−P2 158.60(9) [159.03(6)]; P3−Pt2−Pt1 156.39(7) [156.55(6)]; P4−Pt2−Pt1 109.64(7) [110.10(4)]; P2−Pt2−Pt1 49.62(6) [49.76(4)]; P3−Pt2−H 166.9 [168.0]; P4−Pt2−H 77.4 [77.6]; P2−Pt2−H 82.0 [82.3].

cleaved by methanol,[36] this result suggests the presence of a strong interaction of the type POH···Cl^-.

Crystal Structures of 3 and 4. Crystals of **3** and **4** suitable for X-ray diffraction were obtained from CH_2Cl_2/*n*-hexane. Complexes **3**·$3CH_2Cl_2$ and **4**·$3CH_2Cl_2$ are isomorphous crystallizing in the triclinic space group $P\bar{1}$; the following discussion of the molecular geometry refers to **3**·$3CH_2Cl_2$, with values for **4**·$3CH_2Cl_2$ appended in square brackets for comparison. Each asymmetric unit consists of a complex molecule and three molecules of CH_2Cl_2, the solvent of crystallization. The molecular structure of **3** is depicted in Figure 5; a displacement ellipsoid plot of **4** is provided in the Supporting Information, Figure S24.

In complex **3**·$3CH_2Cl_2$ [complex **4**·$3CH_2Cl_2$] the two Pt atoms are linked by a metal−metal bond of 2.8778(15) [2.8379(4)] Å and bridged by a phosphanide subtending a Pt−P−Pt angle of 77.82(8) [77.71(6)]°. The elongation of the Pt−Pt distance caused by protonation [the Pt−Pt interatomic distance for **1** is 2.5731(16) Å] is consistent with the transformation of the *2e-2c* into a weaker *2e-3c* M−M bond.[40] The presence of the Pt−Pt bond is in line with a valence electron count of 30 and of a Framework Electron Count of 6.[41] The coordination around the Pt atoms is planar with a deviation of the metal from the coordination plane of 0.0625(3) [0.0629(3)] Å for Pt^1 and 0.0350(4) [0.0108(3)] Å for Pt^2. The coordination planes around each platinum are almost coplanar with a dihedral angle of 8.70(9) [7.61(7)]°. The P−H bond of the P^1HCy_2 points toward the bridging phosphanide, while the P−H bond of the P^3HCy_2 points toward the $P^4(OH)Cy_2$, forming an intramolecular hydrogen bond (see Figures 5 and Supporting Information, Figure S24) with the oxygen. A hydrogen bond is present also between the Cy_2P^4OH hydrogen and the neighboring symmetry equivalent Cl^- [Br^-] counteranion, thus corroborating our deductions on POH···Cl^- interactions in solution stemming from ^{35}Cl NMR experiments. Table 1 shows the main features of the hydrogen bonds for both structures. Passing from chloride to bromide acceptors the hydrogen-bond distance increases by 0.15 Å.[42] The O···Cl and H···Cl distances found for **3**·$3CH_2Cl_2$ are comparable to those found in the crystal structure of [Pt(COMe)(PPh_3){(*R,S*)-Ph(HO)PCH_2CH_2P(OH)Ph}]Cl.[43]

Table 1. Interatomic Distances (Å) and Angles (deg) for D−H···A Hydrogen Bonds

D−H···A moiety	D−H	H···A	D···A	D−H···A
O1−H1a[a]···Cl2 for **3**·$3CH_2Cl_2$	0.98	2.12	2.961(8)	143
P3−H3···O1 for **3**·$3CH_2Cl_2$	1.32	2.28	3.266(8)	128
O1−H1a[a]···Br2 for **4**·$3CH_2Cl_2$	0.98	2.27	3.100(5)	141
P3−H3···O1 for **4**·$3CH_2Cl_2$	1.32	2.22	3.190(6)	127

[a] H1a is related to H1 by the symmetry operation *x*, −1 + *y*, *z*.

Synthesis of Neutral Complexes by Reactions with HX (X = Cl, Br). When exactly 1 equiv of HCl or HBr was taken up by complex **1**, the neutral hydrido bridged complexes **5** or **6** containing the $POCy_2$ ligand instead of the $P(OH)Cy_2$ formed (Scheme 2). Passing from $P(OH)Cy_2$ in **3**−**4** to $POCy_2$ in **5**−**6** caused a high-field shift of the ^{31}P NMR signal of about 40 ppm. (Supporting Information, Figures S6 and S9). The hydride ^1H NMR signals of the neutral complexes **5** and **6** (Supporting Information, Figures S7 and S10) are low-field shifted with respect to those of their cationic analogues **3** and **4**.

In the IR spectrum the bands of Pt-μH, P−H and P═O stretchings are located at ν = 1611, 2322, 1088 +1019 cm^{-1} for **5** and ν = 1589, 2324, 1086 +1020 cm^{-1} for **6**. The Pt−Cl band of **5** was found at 285 cm^{-1}.

Complexes **5**−**6** always coexist with variable amounts of **3**−**4** present when reactions are carried out with less than 2 equiv of hydrohalic acid. In these cases an equilibrium between the neutral and the cationic forms was ascertained by $^{31}P\{^1H\}$ exchange spectroscopy (EXSY) experiments. Figure 6 shows the $^{31}P\{^1H\}$ EXSY spectrum of a mixture of the chloro species **3** and **5**. A similar equilibrium between the neutral dimethylphosphinito complex [$(CO)_3$Mn(CNR)-(PMe_3)($POMe_2$)] and its protonated form has been recently described.[44]

Pure **5**−**6** could be obtained by deprotonation of the cationic counterparts **3**−**4** with aqueous NaOH in CH_2Cl_2 (or, alternatively, with NaH in toluene). Interestingly, excess

(39) Spek, A. L. *J. Appl. Crystallogr.* **2003**, *36*, 7–13.
(40) See ref 3 and refs therein.
(41) Aullon, G.; Alemany, P.; Alvarez, S. *J. Organomet. Chem.* **1994**, *478*, 75–82.
(42) Steiner, T. *Acta Crystallogr.* **1998**, *B54*, 456–463.
(43) Powell, J.; Horvath, M. J.; Lough, A. *J. Chem. Soc., Dalton Trans.* **1996**, 1679–1685.

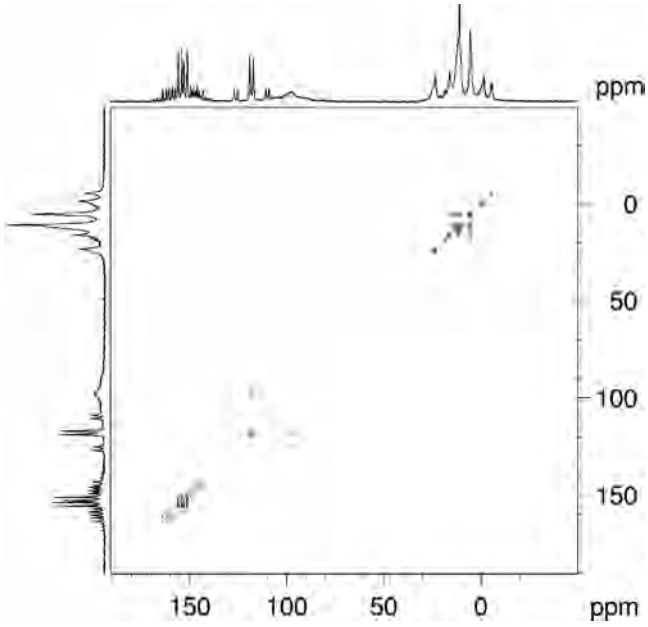

Figure 6. $^{31}P\{^1H\}$ EXSY spectrum (C_6D_6, 295 K) of the mixture of **3** and **5**.

of base and prolonged reaction times caused a further dehydrohalogenation that eventually led to complex **1** (Scheme 2).

Although deprotonation of bridging hydrido complexes has been reported for Co_2,[45] Rh_2,[46] Mo_2,[47] Mo−Mn,[48] Os_3,[49] Mo−Pt or W−Pt[50] systems, to the best of our knowledge no example is known to date of a reversible protonation of a Pt−Pt bond.[51] Such a behavior may be favored in the present case by the possibility of the phosphinite to rebind the Pt^1 restoring the κ^2-*P,O* bridge. The acidity of **5**−**6** corroborates the view of the Pt−H−Pt moiety as a protonated Pt^I−Pt^I fragment rather than a "true" Pt^{II}−Pt^{II} μ-hydride.[52]

Reaction with HI. The reactivity of **1** toward HI differs from that observed with HBr or HCl. Carrying out the reaction of **1** with excess aqueous HI in toluene at 25 °C results, after 30 min, in the formation of an unexpected

Scheme 3. Reaction of **1** with Excess HI

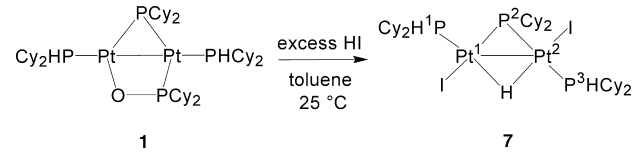

1 **7**

product which was isolated in 70% yield and characterized as the neutral diiodo hydrido-bridged diplatinum complex **7** (see Scheme 3).

The $^{31}P\{^1H\}$ spectrum of complex **7** shows three signals centered at δ 185.7, δ 16.4, and δ 0.9 (Supporting Information, Figure S12). The low field signal is a dd because of a phosphanide bridging two unequivalent Pt atoms ($^1J_{P(2),Pt(1)}$ = 2510 Hz, $^1J_{P(2),Pt(2)}$ = 1919 Hz) having a $PHCy_2$ in *cis* position ($^2J_{P(2),Pt(1)}$ = 6 Hz) and another $PHCy_2$ in *trans* position ($^2J_{P(2),Pt(3)}$ = 321 Hz). Accordingly, **7** shows in the ^1H NMR spectrum a ddd in the hydride region centered at δ −7.29 flanked by three sets of ^{195}Pt satellites from which the $^1J_{H,Pt}$ of 361 (with Pt^1) and 799 Hz (with Pt^2) were extracted (Supporting Information, Figure S13). The values of the ^1H−^{31}P coupling constants (60, 12, and 9 Hz) confirm that only one position *trans* to the hydride is occupied by a P atom ($^2J_{H,P}$ = 60 Hz).

The iodine analogues of complexes **5** and **3** (complexes **8** and **9**, respectively, Scheme 4) were detected by adding gradually $HI_{(aq)}$ to a CD_2Cl_2 solution of **1** in an NMR tube and monitoring the reaction course at 295 K with multinuclear NMR (Supporting Information, Figures S15, S16, S18 and S19).

On standing, complex **9** transforms spontaneously into **10**[53] which, within a few hours, isomerizes completely into the thermodynamically stable complex **7**, namely, the end product found when the reaction between **1** and excess HI was carried out in one pot. The retention of stereochemistry observed in the step **9**→**10** corresponds to the expected outcome for a substitution reaction on a square-planar complex following an associative mechanism.[54] Complex **8** could be isolated in the pure state after reaction of **1** with exactly an equimolar amount of hydroiodic acid. On the other hand, pure **9** was obtained by carrying out the reaction of **1** with 2 equiv of HI in dichloromethane and stopping the reaction as soon as NMR monitoring showed the complete consumption of **8**.

Mechanism of the Reaction. The results presented up to here reveal that the protonation of **1** by HX (X = Cl, Br, I) causes the opening of the phosphinito bridge giving rise to hydrido bridged complexes in which the dicyclohexylphosphinito behaves as monodentate ligand on Pt^2 and the anion of the acid binds to Pt^1.

Knowing that Pt^1 of **1** is susceptible to nucleophilic attack,[3] we have first tried to determine whether the first step of the

(44) Ruiz, J.; Garcia-Granda, S.; Diaz, M. R.; Quesada, R. *Dalton Trans.* **2006**, 4371–4376.
(45) Werner, H.; Hofmann, W.; Zolk, R.; Dahl, L. F.; Kocal, J.; Kühn, A. *J. Organomet. Chem.* **1985**, *289*, 173–188.
(46) (a) Hermann, W. A.; Plank, J.; Ziegler, M. L.; Balbach, B. *J. Am. Chem. Soc.* **1980**, *102*, 5906–5908. (b) Hermann, W. A.; Plank, J.; Riedel, D. *J. Organomet. Chem.* **1980**, *190*, C47–C50. (c) Hermann, W. A.; Plank, J.; Guggolz, M. E.; Ziegler, M. L. *Angew. Chem., Int. Ed. Engl.* **1980**, *19*, 651–653. (d) Hermann, W. A.; Plank, J.; Riedel, D.; Ziegler, M. L.; Weidenhammer, K.; Balbach, B. *J. Am. Chem. Soc.* **1981**, *103*, 63–75.
(47) (a) Petersen, J. L., Jr. *Inorg. Chem.* **1980**, *19*, 186–191. (b) Adatia, T.; McPartlin, M.; Mays, M. J.; Morris, M. J.; Raithby, P. R. *J. Chem. Soc., Dalton Trans.* **1989**, 1555–1564.
(48) Casey, C. P.; Bullock, R. M. *Organometallics* **1984**, *3*, 1100–1104.
(49) Colbran, S. B.; Johnson, B. F. G.; Lewis, J.; Sorrell, R. M. *J. Organomet. Chem.* **1985**, *296*, C1–C5.
(50) Powell, J.; Sawyer, J. F.; Smith, S. J. *J. Chem. Soc., Chem. Commun.,* **1985**, 1312–1313.
(51) A spontaneous dehydrochlorination of the bridging hydrido complex stemming from protonation of $[PtCl(dppm)]_2$] has been described in Brown, M. P.; Puddephatt, R. J.; Rashidi, M.; Seddon, K. R. *J. Chem. Soc., Dalton Trans.* **1978**, 516–522.
(52) Similar conclusions were drawn by a DFT study on the related complex **2**. See ref 3.
(53) Spectroscopic features of **10**: ^1H NMR ($CDCl_3$, δ): 4.71 (m, H(1), $^1J_{H(1),P(1)}$ = 345 Hz, $^2J_{H(1),Pt(1)}$ = 126 Hz), −4.35 (td, H(2), $^2J_{H(2),P(2)}$ = 9 Hz, $^2J_{H(2),P(1)}$ = 80 Hz, $^1J_{H(2),Pt(1)}$ = 436 Hz) ppm. $^{31}P\{^1H\}$ NMR ($CDCl_3$, δ): 171.0 (s, P(2), $^1J_{P(2),Pt(1)}$ = 2663 Hz), −2.4 (s, P(1), $^1J_{P(1),Pt(1)}$ = 3640 Hz, $^2J_{P(1),Pt(1')}$ = 248 Hz, $^3J_{P(1),P(1')}$ = 63 Hz) ppm. $^{195}Pt\{^1H\}$ NMR ($CDCl_3$, δ): −5711 (ddd, Pt(1), $^1J_{Pt(1),P(2)}$ = 3981 Hz, $^1J_{Pt(1),P(1)}$ = 4334 Hz) ppm.

Scheme 4. Reaction Course of **1** with HI

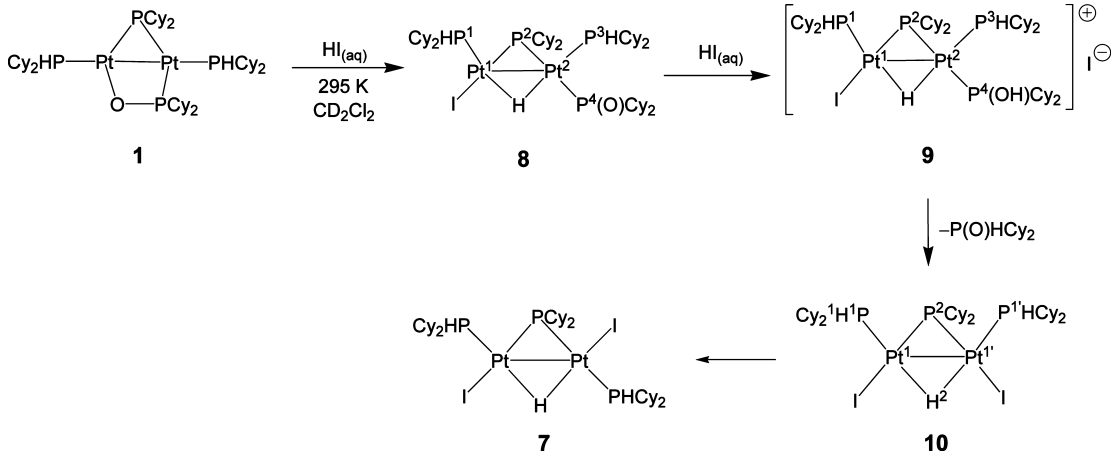

Scheme 5. Possible Pathways for the Protonation of **1**

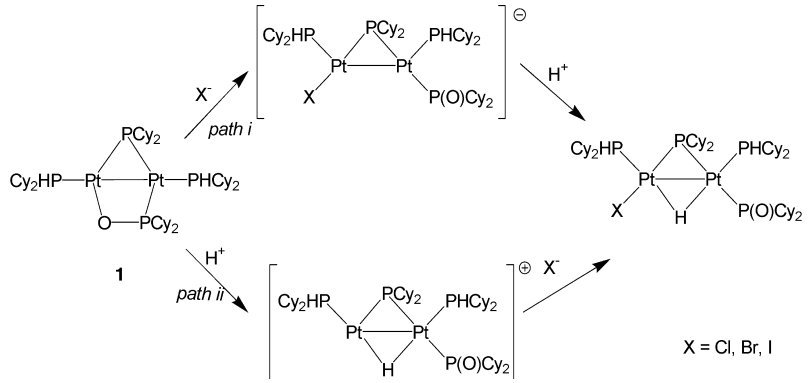

reaction with HX was the attack of the halide on **1**, with opening of the phosphinito bridge and thus rendering the molecule susceptible of proton attack (Scheme 5, path *i*) or whether, alternatively, the reaction started with a proton attack on **1** that results in the formation of the bridging hydride, followed by coordination of the halide to Pt^1 (Scheme 5, path *ii*). The contemporary attack of H^+ and X^- from molecular HX has to be discarded in the light of the effective reaction that occurs when aqueous HX were used.

To discriminate between paths *i* and *ii* we have carried out the following experiments:

(*a*) an equimolar mixture of **1** and $[Bu_4N]Cl$ (chosen to consider the interaction of the chloride with the Pt complex) was stirred in tetrahydrofuran (THF) at room temperature but no changes in the multinuclear NMR spectra of the solution was observed during the 3 days of monitoring. The same result was obtained using a saturated THF solution of NaCl;

(*b*) etherate HBF_4 (having a poorly nucleophilic anion and therefore chosen to consider the interaction of the H^+ with the Pt complex) was added to a *n*-hexane solution of **1** at room temperature causing the immediate transformation into a hydrido bridged dinuclear Pt species characterized by a ^1H NMR signal at δ −5.4 ($^1H-^{195}Pt$ HMQC experiment). The addition of few drops of acetonitrile to the solution allowed us to isolate the complex $[(PHCy_2)(CH_3CN)Pt(\mu\text{-}PCy_2)(\mu\text{-}H)Pt(PHCy_2)\{\kappa P\text{-}P(OH)Cy_2\}](BF_4)_2$ (*Pt−Pt*) (**11**).[55]

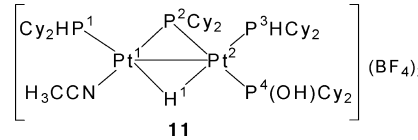

Although the findings described in point *a* do not allow the possibility of discriminating between the incapacity of chloride to open the phosphinito bridge and the establishment of an energetically unfavorable pre-equilibrium between **1** and its (undetected) chloro adduct, the findings reported in point *b* unequivocally indicate path *ii* as operative. In fact the formation of the bridging hydride upon reaction of **1** with HBF_4 demonstrates that the proton can attack **1** without the prior opening of the phosphinito bridge by a nucleophile.

Once it was ascertained that the first act of the reaction is the proton attack on **1**, it remained to establish the site where

(54) Henderson, R. A. *The Mechanisms of Reactions at Transition Metal Sites, Oxford University Press* **1993**, p. 13.

(55) Main spectroscopic features for **11**: ^1H NMR (CD_3CN, δ): −6.48 (m, $^2J_{H(1),P(1)} = 65$ Hz, $^2J_{H(1),P(3)} = 63$ Hz, $^2J_{H(1),P(4)} = 16$ Hz, $^2J_{H(1),P(2)} = 11$ Hz, $^1J_{H(1),Pt(2)} = 516$ Hz, $^1J_{H(1),Pt(1)} = 392$ Hz, μ-H) ppm. $^{31}P\{^1H\}$ NMR (CD_3CN, δ): 155.2 (dd, P(2), $^1J_{P(2),Pt(1)} = 2674$ Hz, $^1J_{P(2),Pt(2)} = 1485$ Hz, $^2J_{P(2),P(4)} = 290$ Hz, $^2J_{P(2),P(3)} = 12$ Hz), 126.7 (dd, P(4), $^1J_{P(4),Pt(2)} = 2764$ Hz, $^2J_{P(4),Pt(1)} = 48$ Hz, $^2J_{P(4),P(2)} = 290$ Hz, $^2J_{P(4),P(3)} = 25$ Hz), 0.6 (d, P(1), $^1J_{P(1),Pt(1)} = 3822$ Hz, $^2J_{P(1),Pt(2)} = 175$ Hz, $^3J_{P(1),P(3)} = 41$ Hz), −2.2 (m, P(3), $^1J_{P(3),Pt(2)} = 3444$ Hz, $^2J_{P(3),Pt(1)} = 179$ Hz, $^2J_{P(3),P(2)} = 12$ Hz, $^2J_{P(3),P(4)} = 25$ Hz, $^3J_{P(3),P(1)} = 41$ Hz) ppm. More details on the reactivity of **1** with HBF_4 will be reported elsewhere.

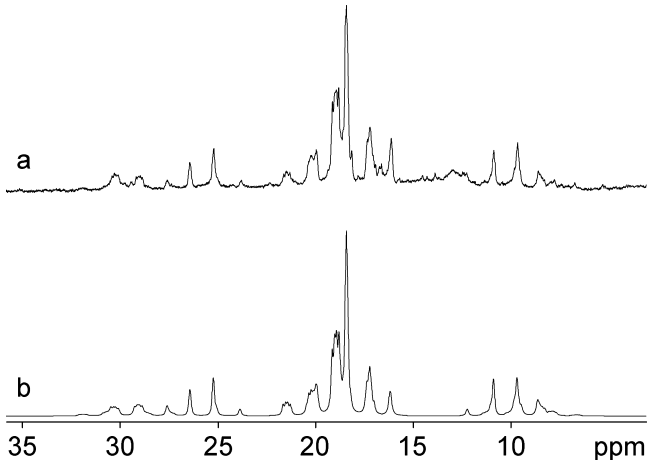

Figure 7. Portion of the $^{31}P\{^1H\}$ NMR spectrum of **12**: (a) experimental; (b) calculated.

H^+ binds. As already mentioned, the incoming proton may first attack (a) the Pt−Pt bond or one of the Pt atoms; (b) a P−Pt bond; and (c) the oxygen atom of the coordinated $POCy_2$. The latter protonation site is that favored by DFT calculations on **1** that indicated the phosphinito oxygen as the most nucleophilic center of the molecule.[3] Moreover, it is known that the small intrinsic barrier typical for protonation at the oxygen often causes protonation of an oxygen ligand to be more facile than protonation of the metal even if the latter (as in the system at hand) is thermodynamically favored.[56] A relevant example of proton attack onto an oxygen atom of a Pt complex has been recently described for the reaction of triflic acid with the triangulo cluster $[Pt_3(\mu\text{-}P^tBu_2)_3(H)(CO)_2]$[57] which proceeds through the formation of a CO-hydrogen bonded (or protonated) intermediate giving a bridging hydride complex as the final thermodynamic product.

Monitoring the reaction between **1** and aqueous HCl (<1 equiv) with ^{31}P and ^1H NMR spectroscopy allowed us to detect, along with unreacted **1** and small amounts of **5**, the formation of an intermediate **12**, which slowly transforms into **5**, and that was found relatively stable at low temperature in toluene (1 week at −10 °C).

The $^{31}P\{^1H\}$ NMR spectrum of intermediate **12** shows four mutually coupled signals, all flanked by ^{195}Pt satellites: a low-field ddd centered at δ 186.9 attributable to a phosphanide bridging two non equivalent Pt atoms, a doublet of pseudotriplets centered at δ 117.1 attributable to a dicyclohexylphosphinito moiety, and a second order set of signals near δ 19 belonging to the two coordinated $PHCy_2$. These latter signals constitute the AB part of the ABXY spin system where A and B are the *P*HCy_2, X is the μ-*P*Cy_2, and Y is the *P*OH. The whole spectrum was calculated (Figure 7), and the spectroscopic features reported in Table 2 were obtained.

The NMR data reported above indicate a structure for **12** in which the position of the P atoms is the same as that in the parent compound **1**, the main difference being the significant deshielding of both the phosphanide P^2 and the phosphinito P^4.

Table 2. NMR Parameters for the Intermediate **12** (C_6D_6, 295 K)[a]

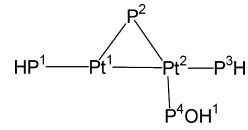

	P^2	P^1	P^4	P^3	Pt^1	Pt^2
P^2	**187.3**	40	251	6	3897	2727
P^1		**19.3**	22	195	3330	520
P^4			**117.5**	8	48	3690
P^3				**19.0**	428	2500
Pt^1					**−4856**	
Pt^2						**−5194**

[a] Chemical shifts (bold typeface) are in ppm; coupling constants (normal type) are in Hz. The drawing represents the skeleton of **12** as inferable from NMR data.

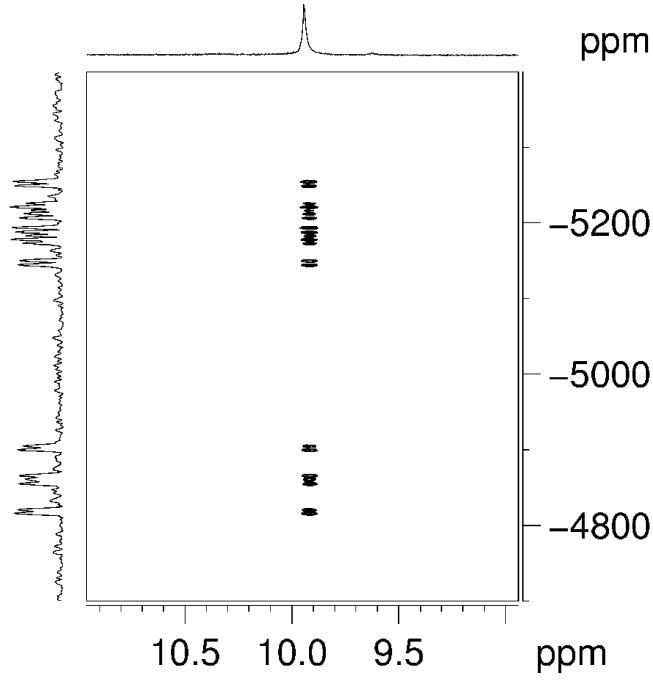

Figure 8. Low field portion of the ^1H-^{195}Pt HMQC spectrum of **12** (C_6D_6, 295 K).

The most interesting feature of the ^1H NMR spectrum of the intermediate **12** (that does not show high-field resonances attributable to hydrides) is a low-field signal centered at δ 10.0 (295 K, C_6D_6). Such a signal refers to a proton which is scalar coupled to both of the Pt atoms, as ascertained by $^1H-^{195}Pt$ HMQC experiment (Figure 8), but to none of the P atoms, a circumstance that suggests the presence of a $PCy_2(OH)$ ligand involved in a cyclic structure.[58] This is in accordance with the remarkable sharpness of the P^4 signal in the $^{31}P\{^1H\}$ NMR and the H^1 signal in the ^1H NMR spectrum of **12**.[59]

The presence of the $P(OH)Cy_2$ moiety in **12** was definitely ascertained by heteronuclear Overhauser enhancement spec-

(56) Kristjansdottir, S. S.; Norton, J. R. *Transition Metal Hydrides*; Dedieu, A. , Ed.; VCH: New York, 1992; pp 309−359; and references cited therein.

(57) Fortunelli, A.; Leoni, P.; Marchetti, L.; Pasquali, M.; Sbrana, F.; Selmi, M. *Inorg. Chem.* **2001**, *40*, 3055–3060.

(58) In the case of $[PtCl(PHCy_2)\{(PCy_2O)_2H\}]$, the proton bound to the phosphinito groups showed a scalar coupling with Pt through Pt−P−O−H bonds but not with the P atoms. See: Mastrorilli, P.; Latronico, M.; Nobile, C. F.; Suranna, G. P.; Fanizzi, F. P.; Englert, U.; Ciccarella, G. *Dalton Trans.* **2004**, 1117–1119.

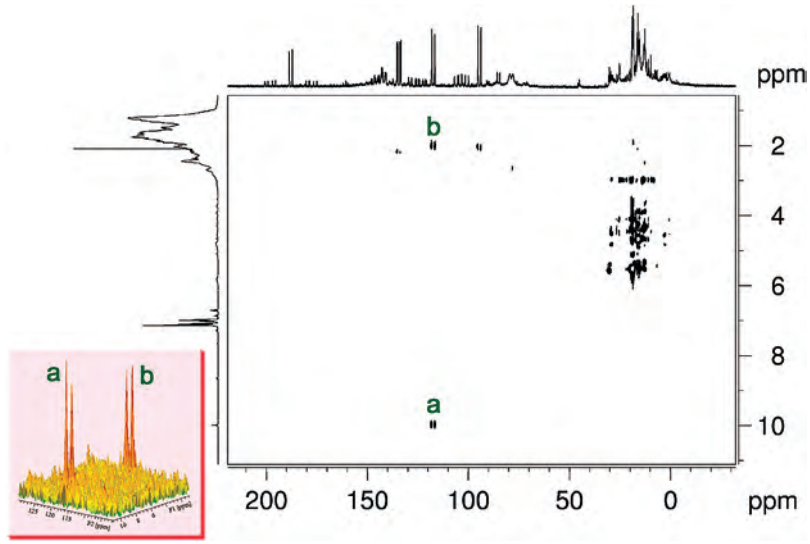

Figure 9. $^{31}P-^{1}H$ HOESY spectrum of a mixture of **12**, **1**, and **5** (C_6D_6, 295 K). The inset shows cross peaks *a* and *b* in a 3D view.

Table 3. NMR Parameters for the Intermediates from the First Attack of HX (X = Cl, Br, I or PhS) on **1**[a]

	HX	δ P^1	δ P^2	δ P^3	δ P^4	δ H^1	δ Pt^1	δ Pt^2
12	$HCl_{(g)}$	19.4	186.9	18.1	117.0	9.9	−4856	−5194
13	$HBr_{(aq)}$	20.1	193.2	18.3	117.5	9.2	−4984[b]	−5179[b]
14	$HI_{(aq)}$	20.1	187.4	19.4	117.4	10.2	−4059	−5195
18[c]	PhSH	17.2	188.0	16.9	109.4	11.7	−5000	−5180

[a] See Table 2 for atom numbering. Solvent C_6D_6; T = 295 K. [b] In CD_2Cl_2. [c] 283 K.

troscopy (HOESY) experiments which showed through space correlations between H and P. The presence of the cross-peak *a* between the signals of H^1 (δ 10.0) and P^4 (δ 117.1) in the $^{31}P-^{1}H$ HOESY (Figure 9) suggests that the acidic proton belongs to a $P(OH)Cy_2$ ligand and that its permanence on the phosphinito group is relatively long (i.e., its involvement in exchange processes, typical for protic species, is slow in the NMR time scale). Moreover, as it is apparent from the box in Figure 9, the comparable volumes of the cross-peaks *a* (between P^4 and H^1) and *b* (between P^4 and the methinic protons of the cyclohexyl groups) indicate that the $P^4\cdots H^1$ distance is compatible with a P−O−H moiety, even though an accurate determination of such distance was not possible.[60]

Intermediates similar to **12** were detected by monitoring at 295 K the protonation of **1** by $HBr_{(aq)}$ (intermediate **13**) or by $HI_{(aq)}$ (**14**) but not when the Brønsted acid was HBF_4 (either aqueous, or etherate,[61] Table 3). This suggests a role of the halide in the formation of intermediates **12**−**14**. To confirm such a role, we have reacted **1** with equimolar

Chart 1

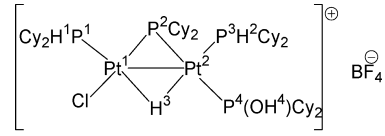

3a

amounts of complexes **3** or **3a** (Chart 1) as protonating agents. Those complexes have the same cation, featuring an acidic proton bound to the PO, and differ only for the counteranion which is a chloride for **3** and a tetrafluoroborate for **3a**. The detection of **12** by monitoring the reaction was possible using **3** but not using **3a** (Table 4) thus definitively pointing out the role played by the chloride in stabilizing the intermediate **12**.

The absence of any signal in the ^{35}Cl NMR spectrum of **12** (see above)[36] rules out structures in which the chloride is purely the counteranion of the protonated form of complex **1**. In other words, the chloride must be either covalently bound or involved in an intimate ion couple.

With the data collected on intermediate **12** the three structures depicted in Scheme 6 can be put forward.

Structure **A** is an ion couple in which the chloride interacts with the acidic proton of the POH ligand; structure **B** features a covalent chloride and the POH ligand involved in a 6-membered metallacycle; structure **C** features a covalently bound chloride and the POH ligand involved in a 4-membered ring.

Structure **A** differs from **B** and **C** in that the halide is not covalently bound to Pt^1. To gain insights into the possible coordination of the X residue of the Brønsted acid HX on Pt^1, we have carried out the reaction of **1** with Brønsted acids having a residue containing NMR informative nuclei. The first two molecules tested for this purpose were $HF_{(aq)}$ and 2,2,2-trifluoroethanol, both having a moderate acidity and the fluorine atoms suitable for NMR studies. The addition of an equimolar amount of 2,2,2-trifluoroethanol to **1** in *n*-hexane gave no reaction after 1 week at room temperature.

(59) The $\Delta\nu_{1/2}$ of the $^{31}P\{^{1}H\}$ NMR signal of the coordinated $P(OH)Cy_2$ in complexes **3** and **4** (with the $P(OH)Cy_2$ exhibiting a monodentate behavior) are 52 and 54 Hz respectively, to be compared with the $\Delta\nu_{1/2}$ of the $^{31}P\{^{1}H\}$ NMR signal of the coordinated $P(OH)Cy_2$ in intermediate **12** of 4 Hz. Analogously, in the ^{1}H NMR spectra, the $\Delta\nu_{1/2}$ of PO*H* for the coordinated $P(OH)Cy_2$ in complexes **3** and **4** are 126 and 112 Hz, respectively, to be compared with the $\Delta\nu_{1/2}$ = 6 Hz for intermediate **12**.

(60) An accurate determination of the $P^4\cdots H^1$ distance needs preliminary experiments for the evaluation of T_1 values and kinetic NOE profiles. Such experiments are dramatically time-consuming and incompatible with the relatively short lifetime of **12** at 295 K.

(61) Intermediate **12** was detected also by monitoring the reaction of **1** with gaseous HCl.

Table 4. Role of the Counteranion of the Protonating Agent in the Stabilization of the Intermediate of the First Protonation

protonating agent	$HCl_{(g)}$	$HCl_{(aq)}$	$HBr_{(g)}$	$HBr_{(aq)}$	$HI_{(aq)}$	$HBF_{4(aq)}$	$HBF_4 \cdot Et_2O$	**3**	**3a**
detection of intermediates similar to **12**	yes	yes	yes	yes	yes	no	no	yes	no

Scheme 6. Three Possible Structures for Intermediate **12**

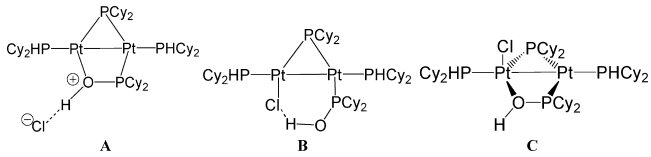

Scheme 7. Reactions of **1** with Phenol and 2,2,2-Trifluoroethanol

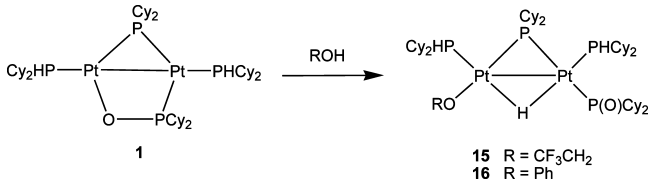

Scheme 8. Reaction Course of **1** with Thiophenol

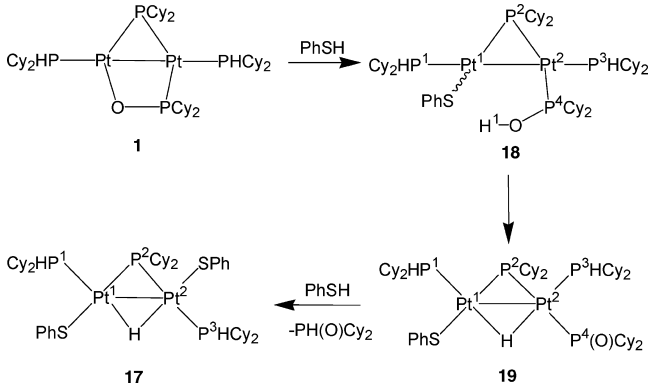

However, using a 10-fold excess of the alcohol resulted in the nearly quantitative formation of **15**[62] after 2 days at room temperature in toluene (Scheme 7). Unfortunately, no intermediates were detected during the monitoring of the reaction. In the case of HF, no reaction occurred even when a strong excess of the acid was used.[63]

The third molecule chosen was phenol, having a residue with aromatic protons for which the scalar coupling with Pt^1 could be easily proven by ^1H-^{195}Pt HMQC experiments. However, results similar to those obtained with 2,2,2-trifluoroethanol were obtained: no intermediates were detected,[64] and the transformation of **1** into **16** (Scheme 7) was achieved after 3 days at room temperature using a 10-fold excess of phenol.

The detection of the intermediate coming from the first attack of the acidic molecule on **1** was possible using PhSH. The reaction of **1** with PhSH led to **17** as the final product, and its course is shown in Scheme 8. The first species detected in solution is intermediate **18** which shows spectroscopic features similar to those of **12** (Table 3). This intermediate collapses into **19** (the thiophenoxide analogues of **5** and **6**), which is present in solution always in small amount. The circumstance that the NMR signals of **19** are broad throughout the reaction indicates that it is involved in a further reaction. In fact, **19** reacts faster than **1** with PhSH giving the neutral hydrido bridged complex **17** containing two coordinated thiophenoxides.[65] As a consequence, even when equimolar amounts of **1** and PhSH were reacted at 0 °C, the final mixture contained mainly **17** with unreacted **1**.

The $^{31}P-^1H$ HOESY spectrum of the reaction mixture containing **18** (along with residual **1**) showed, as in the case of HCl as protonating agent, the cross peak due to the dipolar coupling between the acidic H^1 and the phosphinite P^4. Moreover the $^1H-^{195}Pt$ HMQC spectrum of the reaction mixture containing **18** (Figure 10) showed correlations between (i) the H^1 proton at δ 11.7 (C_6D_6) with *both* Pt atoms, according to what was found for **12**, **13**, and **14**; (ii) the *ortho* protons of the thiophenyl group with the Pt^1 atom. The latter result permits to rule out a structure of type **A** for intermediate **18** and, extending this result to the other protonating agents giving observable intermediates, to **12**, **13**, and **14**. The discrimination between structures **B** and **C** was made on the basis of DFT calculations.

DFT Study. Density functional calculations were performed on several of the considered complexes and the proposed intermediates to study the energetics of the protonation reactions of **1** and to shed light on their mechanism. This study was carried out using models with methyl groups in place of cyclohexyl groups, an approximation previously validated.[3]

Geometrical parameters calculated for complexes **1** and **3**, for which X-ray structures are available, are in good agreement with the experimental data, with bond lengths within 0.1 Å and bond angles within 5°. As to complex **3**,

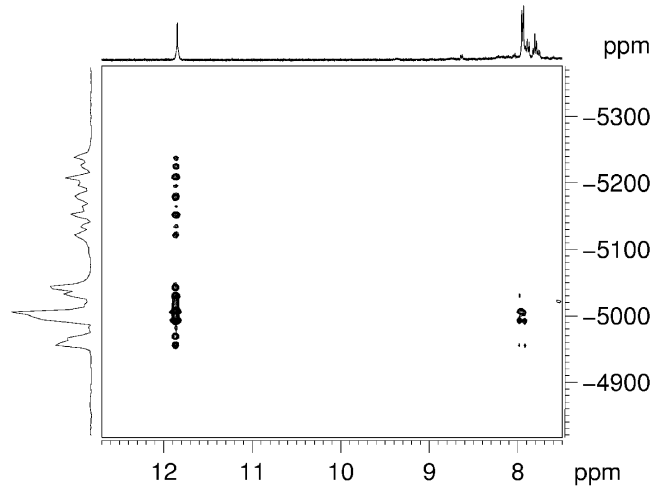

Figure 10. Portion of the ^1H-^{195}Pt HMQC spectrum of the reaction mixture obtained immediately after mixing **1** with PhSH (283 K, C_6D_6). The cross peaks refer to intermediate **18**.

(62) The isolation of **15** was hampered by its decomposition during work-up procedures.

(63) The addition of aqueous HF resulted only in the broadening of the ^{31}P NMR signals of **1**.

(64) The addition of excess phenol (2,2,2-trifluoroethanol) resulted in the broadening of the ^{31}P NMR signals of **1**, which progressively decrease with the appearance of the peaks attributed to **16** (**15**).

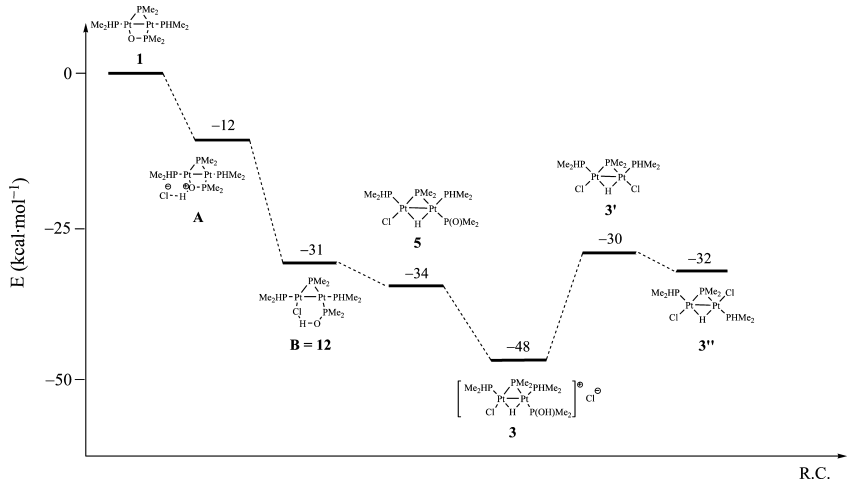

Figure 11. Energy diagram for the protonation reaction of **1** with HCl in *n*-hexane solution.

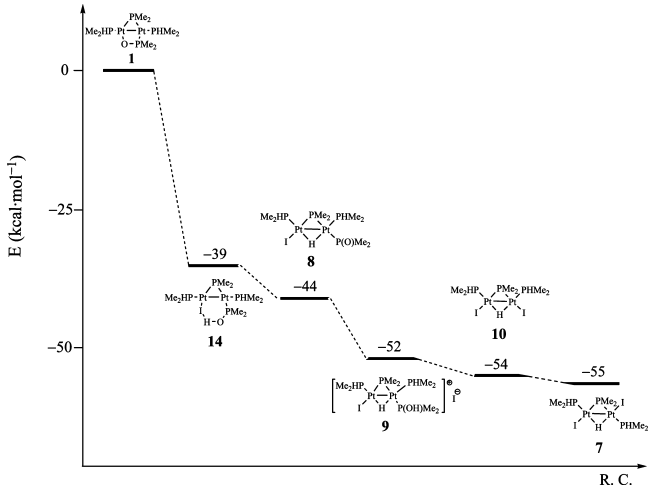

Figure 12. Energy diagram for the protonation reaction of **1** with HI in *n*-hexane solution.

DFT calculations were performed considering explicitly the complex as an ion pair, as indicated by NMR and diffraction results.

Thermodynamics. The protonation reactions of **1** with one and two HCl and HI molecules (considered as representative of Brønsted acids with a hard and a soft anion respectively) were addressed, and the energetics of these reactions are illustrated by the energy profiles reported in Figures 11 and 12.

In both cases all possible products experimentally observed upon protonation by each of the two acids were considered, that is, **8**, **9**, **10**, and **7** for HI and **5**, **3**, and the Cl analogues of **10** and **7** (hereafter **3′** and **3″**) for HCl.

Figure 11 shows an energy gain of 34 kcal mol^{-1} for the protonation of **1** by one HCl molecule, leading to **5**, and of 48 kcal mol^{-1} for the protonation by two HCl molecules, leading to **3**. Slightly more favorable values, −44 and −52 kcal mol^{-1}, are shown in Figure 12 for the protonation energies of the first and second HI molecules leading to **8** and **9**, respectively. Moreover, complexes **10** and **7**, featuring two covalently bound I atoms, are slightly lower in energy than **9**, by 2 and 3 kcal mol^{-1}, respectively (Figure 12), in agreement with the experimental evidence indicating that **9** evolves spontaneously, first to **10** and eventually to **7**. On the contrary, the ion pair **3** was found more stable than the neutral complex **3′** or **3″** by 18 and 16 kcal mol^{-1}, respectively (Figure 11), giving the rationale for why neither **3′** nor **3″** were ever experimentally observed. The lower stability of symmetric compounds **10** and **3′** with respect to the corresponding unsymmetrical ones **7** and **3″** is due to unfavorable steric interactions between the alkyl substituents of the P ligands, as shown by the calculated geometries.

Reaction Mechanism and Intermediates. Theoretical calculations have been carried out to shed light on the detailed mechanism of the protonation reaction of **1** with HCl and to find the energy barriers for all its steps. Several sites of complex **1** can in principle undergo protonation, such as the two platinum atoms, the phosphinito oxygen, the metal−metal bond, and the Pt−P bonds. We first addressed the preliminary approach of HCl to **1** and investigated the formation of hydrogen bond adducts with each of these sites. Geometry optimizations allowed us to locate six stable adducts corresponding to the formation of a hydrogen bond of HCl with the phosphinito oxygen, with each of the two platinum atoms (the HCl molecule lying perpendicular to the platinum coordination planes), with two Pt−P bonds (the HCl molecule lying in the Pt coordination plane and interacting with both the bridging and one of the terminal phosphanido ligands), and with the Pt^1-P (terminal) bond (the HCl molecule lying in the Pt coordination plane trans to the bridging phosphanido ligand). Among them, the thermodynamically most stable adduct is that with a hydrogen bond between HCl and the phosphinito oxygen, **1**·HCl, with a binding energy of 13.5 kcal mol^{-1}. The formation of the hydrogen bond between the oxygen and the proton is reflected by a lengthening of the H−Cl bond, from 1.31 to 1.53 Å, and the short O···Cl distance of 2.79 Å in the final adduct. Slightly higher in energy are the adducts with a hydrogen bond between HCl and the Pt^1 or Pt^2 atoms, **1**·HCl′ and **1**·HCl″, with bonding energies of 9 and 9.5 kcal mol^{-1},

(65) The similar behavior exhibited by HI and PhSH towards **1** [i.e., the formation of neutral complexes featuring a double incorporation of the residues I (to give **7**) and PhS (to give **17**)] can be rationalized with the high affinity to platinum of the "soft" I and PhS residues which replace the "harder" $P(OH)Cy_2$ ligand on Pt^2.

Scheme 9. Possible Ion Pairs **D**−**I** for the Reaction of **1** with HCl[a]

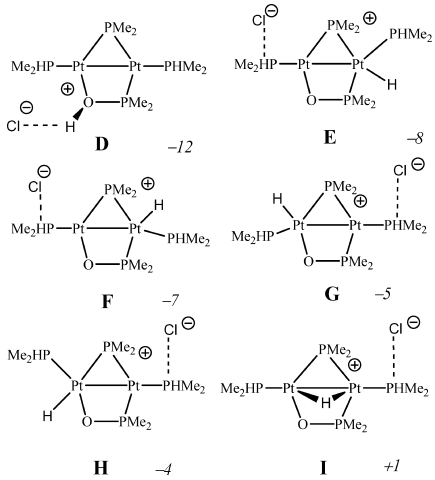

[a] Reaction energies in *n*-hexane solution with respect to **1** + HCl are reported. Structure **D** corresponds to **A**.

respectively, while the adducts in which HCl interacts with the Pt−P bonds are significantly less stable, with binding energies of 4−5 kcal mol^{-1}.

Starting from the calculated hydrogen-bonded adducts, we have studied the thermodynamics of the proton transfer process by optimizing the geometries of the final products. A correct evaluation of the proton transfer from HCl to **1** in the non- or slightly polar solvents employed in the syntheses required to take explicitly into account the formation of an intimate ion couple between the resulting [**1**−H]$^+$ adduct and Cl$^-$.

We thus explicitly considered the most stable ion couples resulting from the proton transfer in each of the above adducts, performing geometry optimizations starting from several Cl$^-$ orientations and evaluating their energies relative to **1** + HCl. Geometry optimizations led only to six minima on the potential energy surface for **1** plus H$^+$ (Scheme 9) corresponding to the protonation of the oxygen atom (**D**), one platinum atom (**E**, **F**, **G**, and **H**), and to the metal−metal bond (**I**). The protonation of one platinum atom or of bridging and terminal Pt−P bonds leads to the terminal hydrido species, E−H, with the H atom lying in the coordination plane. Among them, the thermodynamically most stable ion couple is that with the protonated phosphinito oxygen, **D**, with an energy gain of 12 kcal mol^{-1} with respect to **1** and HCl infinitely apart, while the remaining ion couples are significantly higher in energy, by 4 kcal mol^{-1} or more (Scheme 9).

That the oxygen atom is the most probable site of the initial proton attack can be also rationalized with the concurrence of the following aspects: (i) the O atom has a high negative atomic charge and it is surrounded by the extended region with the most negative electrostatic potential;[3] (ii) the proton approach to O is less hampered by steric hindrance of the large cyclohexyl groups than to the Pt atoms; (iii) there is a significant contribution of p(O) orbitals to the highest occupied molecular orbital (HOMO) of **1**; and (iv) compared with the other mono-protonated structures, the formation of the complexes with protonated O ligand requires the smallest structural changes relative to the parent species **1**.[56]

According to our calculations, the most stable ion couple formed by proton transfer from HCl to **1** corresponds to the structure **A**, one of those initially proposed for intermediate **12** and ruled out on the basis of the experiments with thiophenol (vide supra); combination of experimental and computational data suggests that **A** is an early intermediate of the reaction which rapidly evolves to **12**, in which the Pt−Cl bond has already formed. To assign the structure to the intermediate **12**, detectable in solution by spectroscopic methods, we then carried out geometry optimizations for structures **B** and **C**. While optimization of structure **B** led to a local minimum on the potential energy surface, structure **C** collapsed to **B** when optimized, conceivably because of the instability of the pentacoordination of Pt[1] and the small bonding energy of the protonated phosphinito oxygen to platinum. Structure **B** was found 19 kcal mol^{-1} lower than **A** and lies 31 kcal mol^{-1} below the reactants **1** and HCl and only 3 kcal mol^{-1} above **5** (Figure 11).

It is noteworthy that **A** shows a significant elongation of the Pt−O bond upon oxygen protonation, from 2.18 Å (for **1**) to 2.46 Å, indicative of a high degree of bond weakening. This bond weakening is confirmed by the energy calculation on the structure obtained from **A** upon complete breaking of the Pt−O bond, which showed a negligible (<1 kcal mol^{-1}) energy increase with respect to **A** and indicates a low-energy pathway for the transformation of **A** into **B**. This is confirmed by the energy profile calculated for this step (vide infra) and explains why the early intermediate **A** is not detectable in solution by spectroscopic methods, allowing us, at the same time, to assign structure **B** to intermediate **12** (Figure 11).

Thus far we have considered only the thermodynamics of the proton transfer from HCl to **1**. We will now focus on the kinetic aspects of the proposed mechanism with the aim at finding the energy barrier of the various steps. No barrier is expected for the preliminary formation of the hydrogen bond adduct **1**−HCl, a step whose rate is therefore determined only by diffusion. We then addressed the proton transfer from **1**−HCl to **A**. To estimate the energy barrier we computed the energy profile for this process taking the O−H distance as the reaction coordinate. The O−H distance was varied from 1.26 Å, the value in **1**−HCl, to 1.01 Å, the value found in **A**, optimizing all the remaining geometrical parameters at each fixed value of the O−H distance. The resulting energy profile (Figure 13) indicates that the proton transfer is endothermic by 1.5 kcal mol^{-1} with a low barrier, 2.0 kcal mol^{-1}, showing a maximum only 0.5 kcal mol^{-1} above **A**. We then considered the energy profile for the rearrangement from the initially formed ion pair **A** to the metastable intermediate **12**, taking the Pt−Cl distance as a reaction coordinate. This distance was varied from 3.51 Å, the value in **A**, to 2.42 Å, the value in **12**, optimizing all the remaining geometrical parameters at each fixed value of the reaction coordinate. The energy profile found (Figure 13) indicates for this exothermic process a very low barrier, less

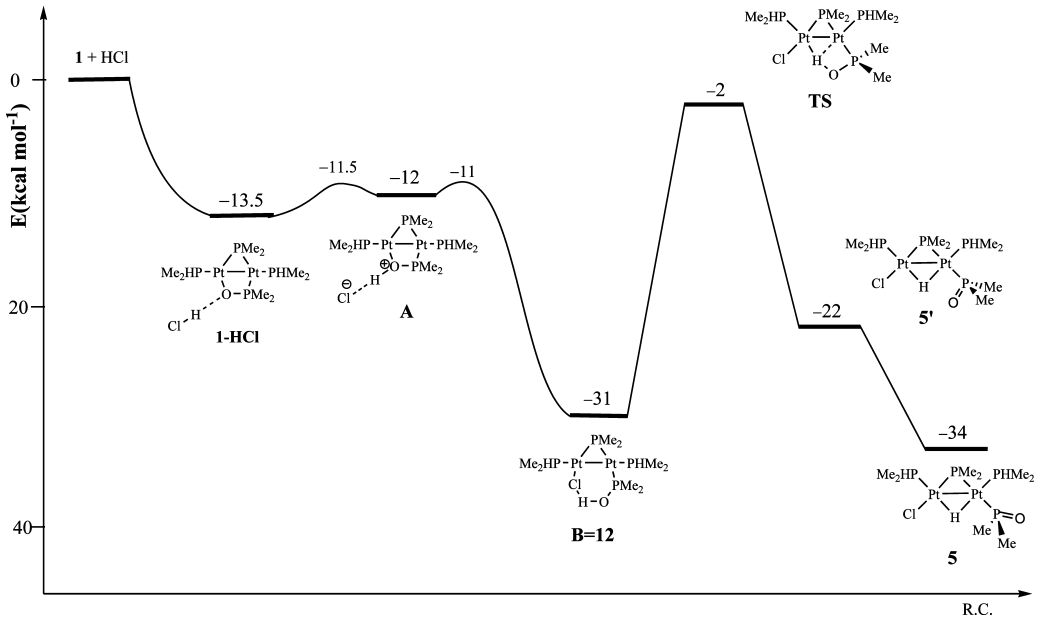

Figure 13. Overall energy profile for the reaction of **1** and HCl to **5**. Reaction energies are reported with respect to **1** + HCl in *n*-hexane solution.

than 1 kcal mol^{-1}, suggesting that **A** is a highly unstable species which evolves immediately to **12**. The formation of the intermediate **12** from **1** + HCl is therefore an extremely fast process with an overall energy barrier of 2 kcal mol^{-1}. Eventually, we considered the energy profile of the intramolecular rearrangement from **12** to **5** (the final product of reaction of **1** with 1 equiv of HCl). In this case, the distance between the oxygen-bound hydrogen and the midpoint of the Pt−Pt bond was taken as the reaction coordinate, which was varied from 3.11 Å, the value in **12**, to 1.08 Å, the final value in **5**, obtaining a maximum in the energy profile about 32 kcal mol^{-1} above **B**. Because the chosen reaction coordinate is only approximate, and the corresponding maximum is quite high, we performed a transition state (TS) search starting from the structure of the maximum. This procedure led to a TS with an energy 29 kcal mol^{-1} above **12** (Figure 13); its structure shows an almost broken O−H bond (1.509 Å), an almost formed Pt^1-H bond (1.829 Å) and a still large Pt^2-H distance of 2.247 Å, and suggests that the high barrier is due to the almost complete breaking of the O−H bond.

The frequency analysis gave an imaginary frequency of 1009 cm^{-1} corresponding to the expected normal mode. Moreover, the energy profile indicates that this transition state is connected to a conformer of **5** with the phosphinito ligand oriented with the oxygen atom directed toward the bridging hydride, **5′**, 12 kcal mol^{-1} above **5**. These results show that the proton transfer from the phosphinito oxygen to the Pt−Pt bond occurs with an energy barrier of 29 kcal mol^{-1} and leads to **5′**, a high energy conformer of **5**, which then relaxes to **5** through a facile rotation around the Pt−P bond. The calculated energy for the intramolecular conversion of the intermediate **12** to **5**, 29 kcal mol^{-1}, is compatible with the experimental evidence of relative stability of this species, that is, 1 week at −10 °C.

Finally, we addressed the second protonation step of **1**, that is, the uptake of an HCl molecule by the first

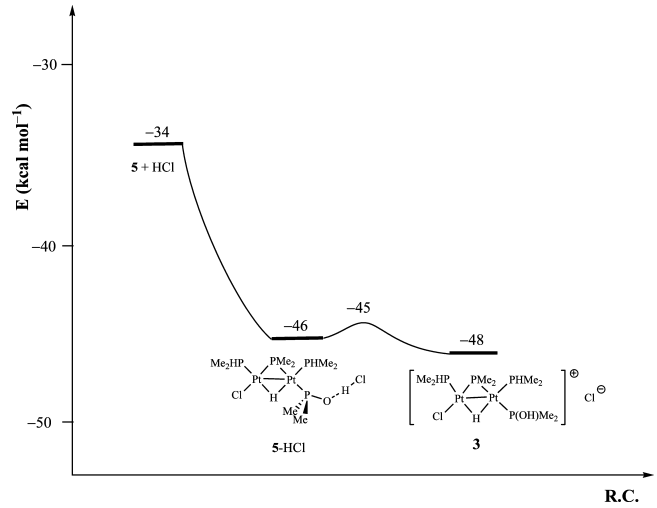

Figure 14. Overall energy profile for the reaction of **5** with HCl to give **3**. Reaction energies are reported with respect to **1** + HCl in *n*-hexane solution.

protonation product **5**. In principle, the protonation sites in **5** are represented by the platinum atoms, the bridging hydride, the Pt−μP bonds, the oxygen, and the chlorine. By considering the interaction of **5** with an HCl molecule, only two stable hydrogen bonded adducts could be found by energy optimization of several starting geometries with all possible orientations of the attacking HCl molecule. These stable hydrogen bound adducts were those having the hydrogen bound to the chlorine or to the oxygen. Their computed bonding energies are 6 and 12 kcal mol^{-1}, respectively, indicating that the hydrogen bond formation to the phosphinito ligand is favored, leading to **5**−HCl (Figure 14). To estimate the energy barrier for the proton transfer from **5**−HCl to the final product **3**, we computed the energy profile taking the O−H distance as the reaction coordinate. The O−H distance was varied from 1.25 Å, the value in **5**−HCl, to 1.01 Å, the value in **3**, optimizing all the remaining geometrical parameters. The energy

profile for the reaction of **5** with HCl to give **3** shown in Figure 14 indicates that the proton transfer step is slightly exothermic, by 2 kcal mol^{-1}, and with a very low barrier, 1.0 kcal mol^{-1}, showing that this is a very easy process, in agreement with the experimental findings.

Conclusions

The amphiphilic character of **1** is demonstrated by its ability to react with both nucleophiles[3] and electrophiles. Reactions of **1** with protic species invariably result in the protonation of the Pt−Pt bond to give unsymmetrical hydrido bridged species. In the case of strong halohydric acids such as HCl or HBr, the products **3**−**6** contain the halide bound to the electrophilic Pt atom. When HI was used as protonating agent, loss of $P(OH)Cy_2$ and incorporation of two iodo ligands in *anti* position led to complex **7**. In the case of weak HX Brønsted acid such as HF, PhOH, CF_3CH_2OH, or PhSH, the feasibility of the protonation of **1** is regulated by the affinity of the conjugated base X^- to the platinum rather than by the strength of the acid. Thus, whereas no reaction occurred with HF, sluggish reactions were observed with PhOH, CF_3CH_2OH, and a fast and complete conversion was obtained with PhSH. The product of the latter reaction (**17**) is the analogue of the diiodo-species **7**, as a result of the high affinity of S and I toward Pt, in view of their "soft" character.

The apparent contrast between the strong nucleophilicity of the phosphinito oxygen indicated by the Mulliken gross atomic charges in **1** and the site selectivity observed in the protonation of **1** (i.e., the addition of the proton to the Pt^I-Pt^I bond) was clarified by a mechanistic study which combined NMR, diffraction methods and theoretical calculations. In fact, it was ascertained that the oxygen atom is indeed the first site of proton attack, provided that a suitable coordinating anion X^- is present in the reaction medium, giving intermediates featuring a six membered $Pt^1-X\cdots H-O-P-Pt^2$ ring. Multinuclear NMR has allowed us to detect such intermediates in solution for derivatives with X = Cl, Br, I, and PhS. The relative stability of the six membered ring intermediates is explainable in terms of a significant energy barrier (29 kcal mol^{-1} for X = Cl) for the proton transfer from the oxygen to the metal−metal bond.

Experimental Section

Complex **1**[2] was prepared as described in ref 3. Gaseous HCl was obtained from NaCl plus concentrated sulfuric acid whereas gaseous HBr was obtained by heating a mixture of NaBr and metaphosphoric acid. All the other reagents were commercial and used as received.

Although the starting complex **1**, as well as all the hydrido bridged products, were found air stable, all manipulations were carried out under a pure dinitrogen atmosphere, using freshly distilled and oxygen-free solvents. C, H, and S elemental analyses were carried out on a Carlo Erba EA1108 CHNS-O Elemental Analyzer. Infrared spectra were recorded on a Bruker Vector 22 spectrometer.

Mass spectrometry analyses were performed using a time-of-flight mass spectrometer equipped with an electrospray ion source (Bruker microTOF). All analyses were carried out in a positive ion mode. The sample solutions were introduced by continuous infusion with the aid of a syringe pump at a flow-rate of 180 μL/min. The instrument was operated at end plate offset −500 V and capillary −4500 V. Nebulizer pressure was 0.8 bar (N_2) and the drying gas (N_2) flow 7 L/min. Capillary exit and skimmer 1 were 90 and 30 V, respectively. Drying gas temperature was set at 220 °C. The software used for the simulations is Bruker Daltonics DataAnalysis (version 3.3).

NMR spectra were recorded on a BRUKER Avance 400 spectrometer; frequencies are referenced to Me_4Si (^1H and ^{13}C), 85% H_3PO_4 (^{31}P), H_2PtCl_6 (^{195}Pt), $CFCl_3$ (^{19}F), and $BF_3\cdot Et_2O$ (^{11}B). The signal attributions and coupling constant assessment was made on the basis of a multinuclear NMR analysis of each compound including, beside 1D spectra, $^1H-^{31}P$ HMQC, $^1H-^{195}Pt$ HMQC, $^{31}P\{^1H\}$ COSY, $^{31}P\{^1H\}$ long-range COSY. The coupling constants not directly extractable from the one-dimensional spectra were obtained and attributed by the tilts of the multiplets due to the "passive" nuclei[66] in the aforementioned 2D spectra. Computer simulation of the $^{31}P\{^1H\}$ NMR spectrum for **12** was performed by using the program WINDAISY (Version 4.0.5.0).

Computational Details. DFT calculations were performed using the Amsterdam density-functional (ADF) package.[67] The 1s orbital for C and O, 1s−2p orbitals for P and Cl, and 1s−4f orbitals for Pt, are kept frozen, respectively. For all main group atoms the valence orbitals were expanded in an uncontracted triple-ζ Slater-type orbitals (STO) basis set augmented with a polarization function. For platinum orbitals we used a double-ζ STO basis set for 5s and 5p and a triple-ζ STO basis set for 5d and 6s. As polarization functions, we used one 6p function for Pt, one 4d for P and Cl, one 3d for C and O and one 2p for H.

The LDA exchange correlation potential was used, together with the Vosko−Wilk−Nusair parametrization[68] for homogeneous electron gas correlation, including the Becke's nonlocal correction[69] to the local exchange expression and Perdew's nonlocal correction[70] to the local expression of correlation energy. Because the relativistic effect is important in these Pt-containing dimers, the zero-order regular approximation formalism (ZORA) without the spin−orbit coupling has been included.[71] Previous calculations indicate that gradient-corrected functionals together with the ZORA approximation can predict reliable properties of metal dimers in comparison with the Dirac four-component-MP2 calculations.[72] Molecular structures of all considered complexes were optimized at this gradient-corrected relativistic level with the above basis set. Single point calculations were subsequently performed on the optimized geometries with a larger basis set obtained from the above one through the addition of a second polarization function, a 5f for Pt, a 4f for P, Cl, C, and O, and one 3d for H. Solvent effects were taken into account employing the COSMO continuum solvent

(66) Carlton, L. *Bruker Report* **2000**, *148*, 28–29.
(67) (a) *Amsterdam Density Functional (ADF)*; SCM, Theoretical Chemistry, Vrije Universiteit: Amsterdam, Netherlands, 2004; www.scm-.com. (b) Boerrigter, P. M.; te Velde, G.; Baerends, E. *J. Int. Quantum Chem.* **1988**, *33*, 87–113. (c) te Velde, G.; Baerends, E. J. *J. Chem. Phys.* **1992**, *99*, 84–98.
(68) Vosko, S. H.; Wilk, L.; Nusair, M. *Can. J. Phys.* **1980**, *58*, 1200–1211.
(69) Becke, A. D. *Phys. Rev. A* **1988**, *38*, 3098–3100.
(70) Perdew, J. P. *Phys. Rev. B* **1986**, *33*, 8822–8824.
(71) (a) Lenthe, E. V.; Baerends, E. J.; Snijders, J. G. *J. Chem. Phys.* **1993**, *99*, 4597–4610. (b) Lenthe, E. V.; Baerends, E. J.; Snijders, J. G. *J. Chem. Phys.* **1994**, *101*, 9783–9792.
(72) (a) Minori, A.; Sayaka, M.; Takahito, N.; Kimihiko, H. *Chem. Phys.* **2005**, *311*, 129–137. (b) Xia, F.; Chen, J.; Cao, Z. X. *Chem. Phys. Lett.* **2006**, *418*, 386–391.

model, [73]in the standard parametrization implemented in the ADF program.[74] Free energies of solvation in *n*-hexane ($\varepsilon = 2.0$) were calculated with the largest basis set on the optimized geometries of all considered molecules.

Syn-[(PHCy$_2$)(Cl)Pt(μ-PCy$_2$)(μ-H)Pt(PHCy$_2$){P(OH)Cy$_2$}]Cl (Pt−Pt) (3). Gaseous HCl was bubbled at room temperature in a toluene solution of **1** (286 mg, 0.239 mmol in 15 mL) causing the progressive discoloration of the initially yellow solution and the contemporary precipitation of **3** as a white solid. The solid was filtered off, washed with *n*-hexane (3 × 4 mL) and dried under reduced pressure.

Yield 278 mg (91%).

The complex is soluble in halogenated solvents, insoluble in toluene and *n*-hexane.

Anal. Calcd for $C_{48}H_{92}Cl_2OP_4Pt_2$: C 45.4, H 7.30; Found C 45.5, H 7.57. HR ESI-MS, exact mass for $C_{48}H_{92}ClOP_4Pt_2$ $[M-Cl]^+$: 1233.5077; measured: *m*/*z*: 1233.5074. The error between simulated and observed isotopic patterns is +0.26 ppm.

IR (KBr, cm^{-1}): $\bar{\nu}$ = 3440 broad w (P−O−H), 2924 s, 2850 s, 2520 m (P−O−H), 2358 w (P−H), 2161 m (P−O−H), 1546 w (Pt−H−Pt), 1495 w, 1447 s, 1340 w, 1324 w, 1294 m, 1263 s, 1206 w, 1179 m, 1106 m, 1005 s, 917 s (P−O−H), 888 m, 847 m, 818 m, 800 m, 734 m, 696 w, 538 w, 523 m, 474 m, 457 w, 407 w, 389 m, 286 m (Pt−Cl).

^{1}H NMR (CD_2Cl_2, δ): 4.58 (m, H(1), $^1J_{H(1),P(1)}$ = 356 Hz, $^2J_{H(1),Pt(1)}$ = 158 Hz), 5.12 (m, H(2), $^1J_{H(2),P(3)}$ = 375 Hz, $^2J_{H(2),Pt(2)}$ = 29 Hz), −5.61 (m, H(3), $^2J_{H(3),P(3)}$ = 74 Hz, $^2J_{H(3),P(1)}$ = 69 Hz, $^2J_{H(3),P(4)}$ = 18 Hz, $^2J_{H(3),P(2)}$ = 14 Hz, $^1J_{H(3),Pt(2)}$ = 568 Hz, $^1J_{H(3),Pt(1)}$ = 389 Hz,), 10.54 (s, H(4)) ppm.^{31}P{^{1}H} NMR (CD_2Cl_2, δ): 155.3 (dd, P(2), $^2J_{P(2),P(4)}$ = 285 Hz, $^2J_{P(2),P(3)}$ = 13 Hz, $^1J_{P(2),Pt(1)}$ = 2597 Hz, $^1J_{P(2),Pt(2)}$ = 1527 Hz), 118.8 (dd, P(4), $^2J_{P(4),P(2)}$ = 285 Hz, $^2J_{P(4),P(3)}$ = 25 Hz, $^1J_{P(4),Pt(2)}$ = 2652 Hz, $^2J_{P(4),Pt(1)}$ = 42 Hz), 10.8 (d, P(1), $^3J_{P(1),P(3)}$ = 50 Hz, $^1J_{P(1),Pt(1)}$ = 4016 Hz, $^2J_{P(1),Pt(2)}$ = 206 Hz), 5.2 (br, P(3), $^3J_{P(3),P(1)}$ = 50 Hz, $^2J_{P(3),P(4)}$ = 25 Hz, $^2J_{P(3),P(2)}$ = 13 Hz, $^1J_{P(3),Pt(2)}$ = 3508 Hz, $^2J_{P(3),Pt(1)}$ = 180 Hz) ppm.

^{195}Pt{^{1}H} NMR (CD_2Cl_2, δ): −5379 (dddd, Pt(1), $^1J_{Pt(1),P(1)}$ = 4016 Hz, $^1J_{Pt(1),P(2)}$ = 2597 Hz, $^2J_{Pt(1),P(3)}$ = 180 Hz, $^2J_{Pt(1),P(4)}$ = 42 Hz, $^1J_{Pt(1),Pt(2)}$ = 845 Hz), −5621 (dddd, Pt(2), $^1J_{Pt(2),P(3)}$ = 3508 Hz, $^1J_{Pt(2),P(4)}$ = 2652 Hz, $^1J_{Pt(2),P(2)}$ = 1527 Hz, $^2J_{Pt(2),P(1)}$ = 206 Hz, $^1J_{Pt(2),Pt(1)}$ = 845 Hz) ppm.

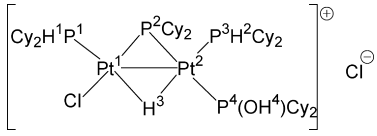

Syn-[(PHCy$_2$)(Cl)Pt(μ-PCy$_2$)(μ-H)Pt(PHCy$_2$){P(OH)Cy$_2$}]-BF$_4$ (Pt−Pt) (3a). Etherate HBF_4 (51÷57%, 38 μL) was added at room temperature under vigorous stirring to a dichloromethane solution of **5** (216 mg, 0.17 mmol in 10 mL). After 10 min the colorless solution was evaporated to dryness, the residue was washed with Et_2O (3 × 4 mL) and *n*-hexane (3 × 4 mL), and dried under reduced pressure. Yield 217 mg (95%).

The complex is soluble in halogenated solvents, insoluble in toluene and *n*-hexane.

Anal. Calcd for $C_{46}H_{92}BClF_4OP_4Pt_2$: C 43.6, H 7.02; Found C 44.1, H 7.15. HR ESI-MS, exact mass for $C_{48}H_{92}ClOP_4Pt_2$ $[M-BF_4]^+$: 1233.5077; measured: *m*/*z*: 1233.5065. (Supporting Information, Figure S2)

IR (KBr, cm^{-1}): $\bar{\nu}$ = 3418 broad w (P−O−H), 3228 broad w, 2926 s, 2850 s, 2661 w, 2336 w (P−H); 1621 w (μ H−Pt); 1447 s; 1349 w; 1327 w, 1300 m; 1179 m; 1077 broad s (BF_4 + PO); 915 s; 886 m; 849 m; 826 w; 771 w; 736 m; 534 s, 522 s; 489 w, 474 m, 409 w, 388 m.

^{1}H NMR (CD_2Cl_2, δ): 4.63 (m, H(1), $^1J_{H(1),P(1)}$ = 357 Hz, $^2J_{H(1),Pt(1)}$ = 156 Hz), 5.00 (m, H(2), $^1J_{H(2),P(3)}$ = 370 Hz, $^2J_{H(2),Pt(2)}$ = 21 Hz), −5.75 (m, H(3), $^2J_{H(3),P(1)}$ = 75 Hz, $^2J_{H(3),P(3)}$ = 66 Hz, $^2J_{H(3),P(2)}$ = 19 Hz, $^2J_{H(3),P(4)}$ = 14 Hz, $^1J_{H(3),Pt(2)}$ = 561 Hz, $^1J_{H(3),Pt(1)}$ = 373 Hz), 9.5 (s, H(4)) ppm.

^{31}P{^{1}H} NMR (CD_2Cl_2, δ): 156.9 (dd, P(2), $^2J_{P(2),P(4)}$ = 286 Hz, $^2J_{P(2),P(3)}$ = 12 Hz, $^1J_{P(2),Pt(1)}$ = 2630 Hz, $^1J_{P(2),Pt(2)}$ = 1538 Hz), 125.1 (dd, P(4), $^1J_{P(4),Pt(2)}$ = 2704 Hz, $^2J_{P(4),Pt(1)}$ = 44 Hz, $^2J_{P(4),P(2)}$ = 286 Hz, $^2J_{P(4),P(3)}$ = 24 Hz), 9.0 (d, P(1), $^1J_{P(1),Pt(1)}$ = 4025 Hz, $^2J_{P(1),Pt(2)}$ = 230 Hz, $^3J_{P(1),P(3)}$ = 50 Hz), 2.6 (br, P(3), $^1J_{P(3),Pt(2)}$ = 3447 Hz, $^2J_{P(3),Pt(1)}$ = 190 Hz, $^2J_{P(3),P(4)}$ = 24 Hz, $^2J_{P(3),P(2)}$ = 12 Hz, $^3J_{P(3),P(1)}$ = 50 Hz) ppm.

^{195}Pt{^{1}H} NMR (CD_2Cl_2, δ): −5375 (dddd, Pt(1), $^1J_{Pt(1),P(1)}$ = 4025 Hz, $^1J_{Pt(1),P(2)}$ = 2630 Hz, $^2J_{Pt(1),P(3)}$ = 190 Hz, $^2J_{Pt(1),P(4)}$ = 44 Hz), −5624 (dddd, Pt(2), $^1J_{Pt(2),P(3)}$ = 3447 Hz, $^1J_{Pt(2),P(4)}$ = 2704 Hz, $^1J_{Pt(2),P(2)}$ = 1538 Hz, $^2J_{Pt(2),P(1)}$ = 230 Hz) ppm.

^{11}B{^{1}H} NMR (CD_2Cl_2, δ): −1.0 (br, BF_4^-).

^{19}F NMR (CD_2Cl_2, δ): −151.6 (br, BF_4^-).

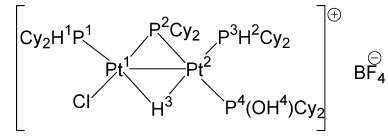

Syn-[(PHCy$_2$)(Br)Pt(μ-PCy$_2$)(μ-H)Pt(PHCy$_2$){P(OH)Cy$_2$}]-Br (Pt−Pt) (4). An aqueous 1.0 M HBr solution (3 mL) was added at room temperature under vigorous stirring to a *n*-hexane solution of **1** (91 mg, 0.08 mmol in 4 mL). After 2 h the organic phase was extracted with *n*-hexane, dried over Na_2SO_4 and filtered to give, after evaporation of the solvent, **4** as a white solid.

Yield 92 mg (91%).

The complex is soluble in halogenated solvents, insoluble in toluene, *n*-hexane.

Anal. Calcd for $C_{48}H_{92}Br_2OP_4Pt_2$: C 42.4, H 6.82; Found C 42.1, H 6.91. HR ESI-MS, exact mass for $C_{48}H_{92}BrOP_4Pt_2$ $[M-Br]^+$: 1277.4572; measured: *m*/*z*: 1277.4517 (Supporting Information, Figure S5).

IR (KBr, cm^{-1}): $\bar{\nu}$ = 3435 broad w (P−O−H), 2923 s, 2850 s, 2655 w, 2580 m (P−O−H), 2360 w (P−H), 2240 w (P−O−H), 1620 w (Pt−H−Pt), 1447 s, 1342 w, 1323 w, 1292 w, 1267 m, 1205 w, 1117 m, 1176 w, 1108 w, 1004 s, 917 s, 898 m, 887 m, 846 m, 816 m, 736 m, 534 w, 522 m, 473 m, 384 w.

^{1}H NMR (CD_2Cl_2, δ): 4.66 (m, H(1), $^1J_{H(1),P(1)}$ = 355 Hz, $^2J_{H(1),Pt(1)}$ = 155 Hz), 5.18 (m, H(2), $^1J_{H(2),P(3)}$ = 374 Hz, $^2J_{H(2),Pt(2)}$ = 37 Hz), −5.51 (m, H(3), $^2J_{H(3),P(3)}$ = 74 Hz, $^2J_{H(3),P(1)}$ = 68 Hz, $^2J_{H(3),P(4)}$ = 16 Hz, $^2J_{H(3),P(2)}$ = 15 Hz, $^1J_{H(3),Pt(2)}$ = 568 Hz, $^1J_{H(3),Pt(1)}$ = 382 Hz), 8.90 (s, H(4)) ppm.

^{31}P{^{1}H} NMR (CD_2Cl_2, δ): 161.7 (dd, P(2), $^2J_{P(2),P(4)}$ = 285 Hz, $^2J_{P(2),P(3)}$ = 13 Hz, $^1J_{P(2),Pt(1)}$ = 2575 Hz, $^1J_{P(2),Pt(2)}$ = 1565 Hz), 120.6 (dd, P(4), $^2J_{P(4),P(2)}$ = 285 Hz, $^2J_{P(4),P(3)}$ = 25 Hz, $^1J_{P(4),Pt(2)}$ = 2675 Hz, $^2J_{P(4),Pt(1)}$ = 43 Hz), 9.6 (d, P(1), $^1J_{P(1),Pt(1)}$ = 3984 Hz, $^2J_{P(1),Pt(2)}$ = 224 Hz, $^3J_{P(1),P(3)}$ = 50 Hz), 4.2 (broad, P(3), $^2J_{P(3),Pt(2)}$ = 3479 Hz, $^2J_{P(3),Pt(1)}$ = 174 Hz, $^3J_{P(3),P(1)}$ = 50 Hz, $^2J_{P(3),P(4)}$ = 25 Hz, $^2J_{P(3),P(2)}$ = 13 Hz) ppm.

^{195}Pt{^{1}H} NMR (CD_2Cl_2, δ): −5522 (dddd, Pt(1), $^1J_{Pt(1),P(1)}$ = 3984 Hz, $^1J_{Pt(1),P(2)}$ = 2575 Hz, $^2J_{Pt(1),P(3)}$ = 174 Hz, $^2J_{Pt(1),P(4)}$ = 43 Hz, $^1J_{Pt(1),Pt(2)}$ = 806 Hz), −5638 (dddd, Pt(2), $^2J_{Pt(2),P(1)}$ = 224 Hz,

(73) Klamt, A.; Schüürmann, G. *J. Chem. Soc., Perkin Trans.* **1993**, *2*, 799–805.

(74) Pye, C. C.; Ziegler, T. *Theor. Chem. Acc.* **1999**, *101*, 396–408.

$^1J_{Pt(2),P(2)}$ = 1565 Hz, $^1J_{Pt(2),P(3)}$ = 3479 Hz, $^1J_{Pt(2),P(4)}$ = 2675 Hz, $^1J_{Pt(2),Pt(1)}$ = 806 Hz) ppm.

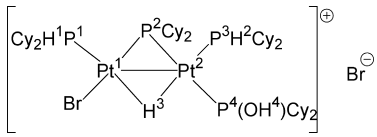

Syn-[(PHCy$_2$)(Cl)Pt(μ-PCy$_2$)(μ-H)Pt(PHCy$_2$){P(O)Cy$_2$}](Pt−Pt) (5). An aqueous 1.5 M NaOH solution (10 mL) was added at room temperature under vigorous stirring to a dichloromethane solution of **3** (222 mg, 0.17 mmol in 15 mL) giving a yellow biphasic system. After 30 min the organic phase was extracted with CH_2Cl_2, dried over Na_2SO_4, and filtered to give, after evaporation of the solvent, **5** as a yellow powder.

Yield 188 mg (87%).

The complex is soluble in halogenated solvents, in toluene, and in *n*-hexane.

Anal. Calcd for $C_{48}H_{91}ClOP_4Pt_2$: C 46.7, H 7.43; Found C 46.6, H 7.28. HR ESI-MS, exact mass for $C_{48}H_{92}ClOP_4Pt_2$: 1233.5082; measured: *m/z*: 1233.5078 $[M+H]^+$ (Supporting Information, Figure S8).

IR (Nujol, cm^{-1}): $\bar{\nu}$ = 2924 s, 2851 s, 2322 w (P−H), 1611 w (Pt−H−Pt), 1447 s, 1377 w, 1343 w, 1261 s, 1177 m, 1088 s (*P* = O), 1019 s (*P* = O), 917 w, 849 m, 803 s, 735 w, 540 w, 520 m, 471 m, 388 m, 285 m (Pt−Cl).

^{1}H NMR (CD_2Cl_2, δ): 4.37 (m, H(1), $^1J_{H(1),P(1)}$ = 349 Hz, $^2J_{H(1),Pt(1)}$ = 160 Hz), 5.12 (m, H(2), $^1J_{H(2),P(3)}$ = 387 Hz, $^2J_{H(2),Pt(2)}$ = 42 Hz), −4.73 (m, H(3), $^2J_{H(3),P(1)}$ = 80 Hz, $^2J_{H(3),P(3)}$ = 70 Hz, $^2J_{H(3),P(2)}$ = 17 Hz, $^2J_{H(3),P(4)}$ = 8 Hz, $^1J_{H(3),Pt(2)}$ = 616 Hz, $^1J_{H(3),Pt(1)}$ = 430 Hz) ppm.

^{31}P{^{1}H} NMR (CD_2Cl_2, δ):145.2 (dd, P(2), $^1J_{P(2),Pt(1)}$ = 2484 Hz, $^1J_{P(2),Pt(2)}$ = 1242 Hz, $^2J_{P(2),P(4)}$ = 268 Hz, $^2J_{P(2),P(3)}$ = 13 Hz), 78.6 (dd, P(4), $^1J_{P(4),Pt(2)}$ = 2328 Hz, $^2J_{P(4),Pt(1)}$ = 56 Hz, $^2J_{P(4),P(2)}$ = 268 Hz, $^2J_{P(4),P(3)}$ = 27 Hz), 16.4 (broad, P(3), $^1J_{P(3),Pt(2)}$ = 3846 Hz, $^2J_{P(3),Pt(1)}$ = 198 Hz, $^3J_{P(3),P(1)}$ = 54 Hz, $^2J_{P(3),P(4)}$ = 27 Hz, $^2J_{P(3),P(2)}$ = 13 Hz), 13.8 (d, P(1), $^1J_{P(1),Pt(1)}$ = 3996 Hz, $^2J_{P(1),Pt(2)}$ = 219 Hz, $^3J_{P(1),P(3)}$ = 54 Hz) ppm.

^{195}Pt{^{1}H} NMR (CD_2Cl_2, δ): −5365 (dddd, Pt(1), $^1J_{Pt(1),P(1)}$ = 3996 Hz, $^1J_{Pt(1),P(2)}$ = 2484 Hz, $^2J_{Pt(1),P(3)}$ = 198 Hz, $^2J_{Pt(1),P(4)}$ = 56 Hz), −5547 (dddd, Pt(2), $^1J_{Pt(2),P(3)}$ = 3846 Hz, $^1J_{Pt(2),P(4)}$ = 2328 Hz, $^1J_{Pt(2),P(2)}$ = 1242 Hz, $^2J_{Pt(2),P(1)}$ = 219 Hz) ppm.

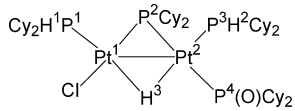

Syn-[(PHCy$_2$)(Br)Pt(μ-PCy$_2$)(μ-H)Pt(PHCy$_2$){P(O)Cy$_2$}](Pt−Pt) (6). Complex **6** was obtained in 79% yield by reaction of **4** with NaOH, following the procedure used for the synthesis of **5**.

The complex is soluble in halogenated solvents, toluene, and *n*-hexane.

Anal. Calcd for $C_{48}H_{91}BrOP_4Pt_2$: C 45.1, H 7.18; Found C 45.0, H 7.21. HR ESI-MS, exact mass for $C_{48}H_{92}BrOP_4Pt_2$ 1277.4577; measured: *m/z*: 1277.4484 $[M+H]^+$ (Supporting Information, Figure S11).

IR (KBr, cm^{-1}): $\bar{\nu}$ = 2924 s, 2848 s, 2656 w, 2347 w, 2324 w (P−H), 1589 w (Pt−H−Pt), 1446 s, 1343 w, 1326 w, 1292 w, 1262 s, 1178 m, 1167 m, 1086 s (*P* = O), 1020 s (*P* = O), 916 w, 901 w, 888 m, 863 m, 848 m, 800 s, 734 w, 539 m, 522 m, 497 w, 454 m, 442 m, 388 m, 285 w.

^{1}H NMR (CD_2Cl_2, δ): 4.61 (m, H(1), $^1J_{H(1),P(1)}$ = 349 Hz, $^2J_{H(1),Pt(1)}$ = 153 Hz), 5.22 (m, H(2), $^1J_{H(2),P(3)}$ = 385 Hz, $^2J_{H(2),Pt(2)}$ = 40 Hz), −4.63 (m, H(3), $^2J_{H(3),P(1)}$ = 77 Hz, $^2J_{H(3),P(3)}$ = 70 Hz, $^2J_{H(3),P(2)}$ = 16 Hz, $^2J_{H(3),P(4)}$ = 7 Hz, $^1J_{H(3),Pt(2)}$ = 520 Hz, $^1J_{H(3),Pt(1)}$ = 441 Hz), ppm.

^{31}P{^{1}H} NMR (CD_2Cl_2, δ): 151.1 (dd, P(2), $^1J_{P(2),Pt(1)}$ = 2465 Hz, $^1J_{P(2),Pt(2)}$ = 1264 Hz, $^2J_{P(2),P(4)}$ = 270 Hz, $^2J_{P(2),P(3)}$ = 13 Hz), 80.3 (dd, P(4), $^1J_{P(4),Pt(2)}$ = 2365 Hz, $^2J_{P(4),Pt(1)}$ = 55 Hz, $^2J_{P(4),P(2)}$ = 270 Hz, $^2J_{P(4),P(3)}$ = 25 Hz), 16.4 (broad, P(3), $^1J_{P(3),Pt(2)}$ = 3808 Hz, $^2J_{P(3),Pt(1)}$ = 225 Hz, $^3J_{P(3),P(1)}$ = 55 Hz, $^2J_{P(3),P(4)}$ = 25 Hz, $^2J_{P(3),P(2)}$ = 13 Hz), 12.7 (d, P(1), $^1J_{P(1),Pt(1)}$ = 3955 Hz, $^2J_{P(1),Pt(2)}$ = 218 Hz, $^3J_{P(1),P(3)}$ = 55 Hz) ppm.

^{195}Pt{^{1}H} NMR (CD_2Cl_2, δ): −5507 (dddd, Pt(1), $^1J_{Pt(1),P(1)}$ = 3955 Hz, $^1J_{Pt(1),P(2)}$ = 2465 Hz, $^2J_{Pt(1),P(3)}$ = 225 Hz, $^2J_{Pt(1),P(4)}$ = 55 Hz, $^1J_{Pt(1),Pt(2)}$ = 950 Hz), −5568 (dddd, Pt(2), $^1J_{Pt(2),P(3)}$ = 3808 Hz, $^1J_{Pt(2),P(4)}$ = 2365 Hz, $^1J_{Pt(2),P(2)}$ = 1264 Hz, $^2J_{Pt(2),P(1)}$ = 218 Hz, $^1J_{Pt(2),Pt(1)}$ = 950 Hz) ppm.

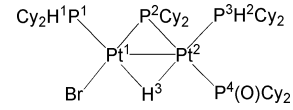

Anti-[(PHCy$_2$)(I)Pt(μ-PCy$_2$)(μ-H)Pt(PHCy$_2$)(I)](Pt−Pt) (7). An aqueous 0.50 M HI solution (0.35 mL) was added at room temperature under vigorous stirring to a toluene solution of **1** (100 mg, 0.084 mmol in 8 mL). After 2 h the organic phase was extracted with toluene, dried over Na_2SO_4, and dried under reduced pressure. The yellow solid was washed with MeOH (3 × 4 mL), *n*-hexane (3 × 4 mL) and dried under reduced pressure.

Yield 82 mg (70%).

The complex is soluble in halogenated solvents and toluene, insoluble in *n*-hexane.

Anal. Calcd for $C_{36}H_{69}I_2P_3Pt_2$: C 34.9, H 5.61; Found C 34.7, H 5.64. HR ESI-MS, exact mass for $C_{36}H_{69}I_2P_3Pt_2Na$: 1261.1889; measured: *m/z*: 1261.1935 $[M+Na]^+$ (Supporting Information, Figure S14).

IR (KBr, cm^{-1}): $\bar{\nu}$ = 2925 s, 2849 s, 2323 w (P−H), 1626 w (Pt−H−Pt), 1462 w, 1448 s, 1341 w, 1329 w, 1290 w, 1262 s, 1195 w, 1175 m, 1106 s, 1023 s, 918 w, 889 w, 854 m, 816 s, 801 s, 731 m, 517 w, 474 m, 391 w.

^{1}H NMR (C_6D_6, δ): 4.64 (m, H(1), $^1J_{H(1),P(1)}$ = 352 Hz, $^3J_{H(1),P(2)}$ = 7 Hz, $^2J_{H(1),Pt(1)}$ = 142 Hz), 5.13 (m, H(2), $^1J_{H(2),P(3)}$ = 347 Hz, $^2J_{H(2),Pt(2)}$ = 10 Hz), −7.29 (m, H(3), $^2J_{H(3),P(1)}$ = 60 Hz, $^2J_{H(3),P(3)}$ = 9 Hz, $^2J_{H(3),P(2)}$ = 12 Hz, $^1J_{H(3),Pt(2)}$ = 799 Hz, $^1J_{H(3),Pt(1)}$ = 361 Hz) ppm.

^{31}P{^{1}H} NMR (C_6D_6, δ): 185.7 (dd, P(2), $^2J_{P(2),P(3)}$ = 321 Hz, $^2J_{P(2),P(1)}$ = 7 Hz, $^1J_{P(2),Pt(1)}$ = 2510 Hz, $^1J_{P(2),Pt(2)}$ = 1919 Hz), 0.6 (broad s, P(1), $^1J_{P(1),Pt(1)}$ = 4255 Hz, $^2J_{P(1),P(2)}$ = 447 Hz, $^2J_{P(1),P(2)}$ = 7 Hz), 16.4 (d, P(3), $^1J_{P(3),Pt(2)}$ = 2463 Hz, $^2J_{P(3),Pt(1)}$ = 41 Hz, $^2J_{P(3),P(2)}$ = 321, Hz) ppm.

^{195}Pt{^{1}H} NMR (C_6D_6, δ): −5723 (ddd, Pt(1), $^1J_{Pt(1),P(1)}$ = 4255 Hz, $^1J_{Pt(1),P(2)}$ = 2510 Hz, $^2J_{Pt(1),P(3)}$ = 41 Hz, $^1J_{Pt(1),Pt(2)}$ = 1365 Hz), −5550 (ddd, Pt(2), $^1J_{Pt(2),P(3)}$ = 2463 Hz, $^1J_{Pt(2),P(2)}$ = 1919 Hz, $^2J_{Pt(2),P(1)}$ = 447 Hz, $^1J_{Pt(2),Pt(1)}$ = 1365 Hz) ppm.

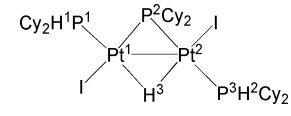

Reaction of 1 with CF_3CH_2OH and PhOH. Solid **1** (100 mg, 0.084 mmol) was added to a toluene solution of CF_3CH_2OH (65 μL, 0.84 mmol in 5 mL) and stirred at room temperature for 2 days, a time after which ^{31}P{^{1}H} NMR monitoring showed the nearly complete conversion of **1** into **15**. An analogous procedure was followed for the reaction of **1** with PhOH that gave >95%

yield of **16** (based on ^{31}P NMR integrals) after 1 day. Attempts to isolate **15** and **16** in pure state were unsuccessful mainly because of the formation of undesired products during the removal of excess CF_3CH_2OH (or phenol).

Spectroscopic Features of **15**:

^1H NMR (C_6D_6, δ): 4.32 (m, H(1), $^1J_{H(1),P(1)} = 335$ Hz, $^2J_{H(1),Pt(1)} = 156$ Hz), 5.21 (m, H(2), $^1J_{H(2),P(3)} = 362$ Hz), −4.32 (m, H(3), $^2J_{H(3),P(1)} = 79$ Hz, $^2J_{H(3),P(3)} = 73$ Hz, $^2J_{H(3),P(2)} = 16$ Hz, $^2J_{H(3),P(4)} = 8$ Hz, $^1J_{H(3),Pt(2)} = 602$ Hz, $^1J_{H(3),Pt(1)} = 431$ Hz) ppm.

$^{31}P\{^1H\}$ NMR (C_6D_6, δ): 143.2 (dd, P(2), $^2J_{P(2),P(4)} = 271$ Hz, $^2J_{P(2),P(3)} = 11$ Hz, $^1J_{P(2),Pt(1)} = 2520$ Hz, $^1J_{P(2),Pt(2)} = 1248$ Hz), 83.9 (dd, P(4), $^1J_{P(4),Pt(2)} = 2410$ Hz, $^2J_{P(4),Pt(1)} = 64$ Hz, $^2J_{P(4),P(2)} = 271$ Hz, $^2J_{P(4),P(3)} = 25$ Hz), 12.5 (d, P(1), $^1J_{P(1),Pt(1)} = 4004$ Hz, $^2J_{P(1),Pt(2)} = 214$ Hz, $^3J_{P(1),P(3)} = 51$ Hz), 13.8 (broad, P(3), $^1J_{P(3),Pt(2)} = 3687$ Hz, $^2J_{P(3),Pt(1)} = 206$ Hz, $^3J_{P(3),P(1)} = 54$ Hz, $^2J_{P(3),P(4)} = 25$ Hz, $^2J_{P(3),P(2)} = 11$ Hz) ppm.

$^{195}Pt\{^1H\}$ NMR (C_6D_6, δ): −5358 (dddd, Pt(1), $^1J_{Pt(1),P(1)} = 4004$ Hz, $^1J_{Pt(1),P(2)} = 2520$ Hz, $^2J_{Pt(1),P(3)} = 206$ Hz, $^2J_{Pt(1),P(4)} = 64$ Hz), −5585 (dddd, Pt(2), $^1J_{Pt(2),P(3)} = 3687$ Hz, $^1J_{Pt(2),P(4)} = 2410$ Hz, $^1J_{Pt(2),P(2)} = 1248$ Hz, $^2J_{Pt(2),P(1)} = 214$ Hz) ppm.

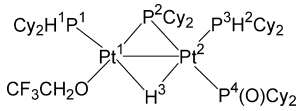

Spectroscopic Features of **16**:

^1H NMR ($CDCl_3$, δ): 7.09 (t, H-*meta*, $^2J_{H,H} = 8$ Hz), 6.83 (d, H-*ortho*, $^2J_{H,H} = 8$ Hz), 6.57 (t, H-*para*, $^2J_{H,H} = 7$ Hz); 4.63 (m, H(1), $^1J_{H(1),P(1)} = 356$ Hz, $^2J_{H(1),Pt(1)} = 156$ Hz, $^3J_{H(1),P(2)} = 5$ Hz), 5.03 (m, H(2), $^1J_{H(2),P(3)} = 368$ Hz, $^2J_{H(2),Pt(2)} = 58$ Hz), −4.97 (m, H(3), $^2J_{H(3),P(1)} = {}^2J_{H(3),P(3)} = 74$ Hz, $^2J_{H(3),P(2)} = 16$ Hz, $^2J_{H(3),P(4)} = 9$ Hz, $^1J_{H(3),Pt(2)} = 599$ Hz, $^1J_{H(3),Pt(1)} = 459$ Hz) ppm.

$^{31}P\{^1H\}$ NMR ($CDCl_3$, δ): 124.9 (dd, P(2), $^2J_{P(2),P(4)} = 276$ Hz, $^2J_{P(2),P(3)} = 16$ Hz, $^1J_{P(2),Pt(1)} = 2470$ Hz, $^1J_{P(2),Pt(2)} = 1205$ Hz), 88.4 (broad d, P(4), $^1J_{P(4),Pt(2)} = 2497$ Hz, $^2J_{P(4),P(2)} = 276$ Hz), 9.5 (d, P(1), $^1J_{P(1),Pt(1)} = 4176$ Hz, $^2J_{P(1),Pt(2)} = 227$ Hz), 9.8 (m, P(3), $^1J_{P(3),Pt(2)} = 3678$ Hz, $^2J_{P(3),P(2)} = 16$ Hz) ppm.

$^{195}Pt\{^1H\}$ NMR ($CDCl_3$, δ): −5177 (dd, Pt(1), $^1J_{Pt(1),P(1)} = 4176$ Hz, $^1J_{Pt(1),P(2)} = 2470$ Hz), −5497 (dddd, Pt(2), $^2J_{Pt(2),P(1)} = 227$ Hz, $^1J_{Pt(2),P(2)} = 1205$ Hz, $^1J_{Pt(2),P(3)} = 3678$ Hz, $^1J_{Pt(2),P(4)} = 2497$ Hz) ppm.

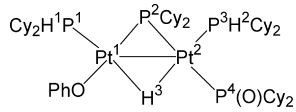

Anti-[(PHCy$_2$)(PhS)Pt(μ-PCy$_2$)(μ-H)Pt(PHCy$_2$)(SPh)] (Pt−Pt) (17). A toluene solution of PhSH (22.1 mg, 0.20 mmol in 4 mL) was added dropwise at room temperature to a stirred toluene solution of **1** (120 mg, 0.10 mmol in 10 mL) giving an orange solution. After 2 h the solvent was removed under reduce pressure, and the obtained solid was treated with MeOH (3 mL). The resulting suspension was filtered, and the yellow-orange solid was washed with MeOH and dried under vacuum. Yield 95 mg (79%).

The complex is soluble in toluene and halogenated solvents, insoluble in methanol.

Anal. Calcd for $C_{48}H_{79}P_3Pt_2S_2$: C 47.9, H 6.62, S 5.33; Found C 47.7, H 6.76, S 5.28.

HR ESI-MS, exact mass for $C_{48}H_{79}P_3Pt_2S_2$: 1202.4131; measured: *m*/*z*: 1202.4132 $[M]^+$ (Supporting Information, Figure S23) and 1093.4087 $[M-PhS]^+$.

IR (KBr, cm^{-1}): $\bar{\nu}$ = 3057 m (aromatic CH), 2923 s, 2847 s, 2331 m (P−H), 2324 m (P−H), 1619 w (Pt−H−Pt), 1576 s, 1468 m,1446 s, 1343 w, 1293 w, 1264 m, 1193 w, 1179 m, 1121 m, 1108 s, 1084 w, 1023 s, 1002 s, 906 m, 861 m, 848 m, 838 m, 817 m, 747 s, 733 s, 697 s, 514 m, 473 s.

^1H NMR (CD_2Cl_2, δ): 7.42/6.86 (m, 10 H, aromatic), 4.79 (m, H(1), $^1J_{H(1),P(1)} = 355$ Hz, $^3J_{H(1),P(2)} = 10$ Hz, $^2J_{H(1),Pt(1)} = 110$ Hz), 3.09 (m, H(2), $^1J_{H(2),P(3)} = 346$ Hz, $^2J_{H(2),Pt(2)} = 13$ Hz), −8.81 (m, H(3), $^2J_{H(3),P(1)} = 69$ Hz, $^2J_{H(3),P(3)} = 13$ Hz, $^2J_{H(3),P(2)} = 11$ Hz, $^1J_{H(3),Pt(2)} = 595$ Hz, $^1J_{H(3),Pt(1)} = 440$ Hz) ppm.

$^{31}P\{^1H\}$ NMR (CD_2Cl_2, Supporting Information, Figure S20, δ): 154.1 (d, P(2), $^2J_{P(2),P(3)} = 298$ Hz, $^1J_{P(2),Pt(1)} = 2050$ Hz, $^1J_{P(2),Pt(2)} = 1975$ Hz), 4.5 (d, P(1), $^1J_{P(1),Pt(1)} = 4046$ Hz, $^2J_{P(1),Pt(2)} = 275$ Hz, $^3J_{P(1),P(3)} = 8$ Hz), 20.8 (d, P(3), $^1J_{P(3),Pt(2)} = 2528$ Hz, $^2J_{P(3),Pt(1)} = 32$ Hz, $^2J_{P(3),P(2)} = 298$ Hz, $^3J_{P(3),P(1)} = 8$ Hz) ppm.

$^{195}Pt\{^1H\}$ NMR (CD_2Cl_2, δ): −5432 (ddd, Pt(1), $^1J_{Pt(1),P(1)} = 4046$ Hz, $^1J_{Pt(1),P(2)} = 2050$ Hz, $^2J_{Pt(1),P(3)} = 32$ Hz), −5465 (ddd, Pt(2), $^1J_{Pt(2),P(3)} = 2528$ Hz, $^1J_{Pt(2),P(2)} = 1975$ Hz, $^2J_{Pt(2),P(1)} = 275$ Hz) ppm.

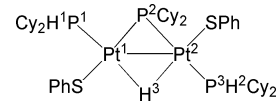

Syn-[(PHCy$_2$)(I)Pt(μ-PCy$_2$)(μ-H)Pt(PHCy$_2$){P(O)Cy$_2$}] (Pt−Pt) (8). Strictly equimolar amounts of HI and **1** were used in this preparation. An aqueous 0.10 M HI solution (0.84 mL) was added at room temperature under vigorous stirring to a dichloromethane solution of **1** (100 mg, 0.084 mmol in 8 mL). After 12 h the organic phase was separated, dried over Na_2SO_4 and filtered. Pure **8** was obtained as a pale yellow powder after evaporation of the solvent. Yield 86 mg (78%).

The complex is soluble in toluene and halogenated solvents.

Anal. Calcd for $C_{48}H_{91}IOP_4Pt_2$: C 43.5, H 6.92; Found C 43.4, H 6.84.

HR ESI-MS, exact mass for $C_{48}H_{91}IOP_4Pt_2$: 1324.4360; measured: *m*/*z*: 1324.4429 $[M]^+$ (Supporting Information, Figure S17).

IR (KBr, cm^{-1}): $\bar{\nu}$ = 2924 s, 2849 s, 2660 w, 2321 w (P−H), 1624 w (Pt−H−Pt), 1447 s, 1345 w, 1327 w, 1292 w, 1263 s, 1194 w, 1178 m, 1089 s (*P* = O), 1023 s (*P* = O), 915 w, 886 w, 849 s, 817 s, 801 s, 734 m, 540 w, 521 m, 468 m, 385 m.

^1H NMR (CD_2Cl_2, δ): 4.50 (m, H(1), $^1J_{H(1),P(1)} = 362$ Hz, $^2J_{H(1),Pt(1)} = 133$ Hz), 5.11 (m, H(2), $^1J_{H(2),P(3)} = 384$ Hz), −4.89 (m, H(3), $^2J_{H(3),P(3)} = 76$ Hz, $^2J_{H(3),P(1)} = 69$ Hz, $^2J_{H(3),P(2)} = 15$ Hz, $^2J_{H(3),P(4)} = 8$ Hz, $^1J_{H(3),Pt(2)} = 671$ Hz, $^1J_{H(3),Pt(1)} = 506$ Hz) ppm.

$^{31}P\{^1H\}$ NMR (CD_2Cl_2, δ): 157.38 (dd, P(2), $^2J_{P(2),P(4)} = 272$ Hz, $^2J_{P(2),P(3)} = 9$ Hz, $^1J_{P(2),Pt(1)} = 2381$ Hz, $^1J_{P(2),Pt(2)} = 1291$ Hz), 81.24 (dd, P(4), $^1J_{P(4),Pt(2)} = 2421$ Hz, $^2J_{P(4),Pt(1)} = 52$ Hz, $^2J_{P(4),P(2)} = 272$ Hz, $^2J_{P(4),P(3)} = 25$ Hz), 9.95 (d, P(1), $^1J_{P(1),Pt(1)} = 3904$ Hz, $^2J_{P(1),Pt(2)} = 295$ Hz, $^3J_{P(1),P(3)} = 53$ Hz), 13.88 (broad, P(3), $^1J_{P(3),Pt(2)} = 3626$ Hz, $^2J_{P(3),Pt(1)} = 201$ Hz, $^3J_{P(3),P(1)} = 53$ Hz, $^2J_{P(3),P(4)} = 25$ Hz, $^2J_{P(3),P(2)} = 9$ Hz) ppm.

$^{195}Pt\{^1H\}$ NMR (CD_2Cl_2, δ): −5745 (dddd, Pt(1), $^1J_{Pt(1),P(1)} = 3904$ Hz, $^1J_{Pt(1),P(2)} = 2381$ Hz, $^2J_{Pt(1),P(3)} = 201$ Hz, $^2J_{Pt(1),P(4)} = 52$ Hz), −5582 (dddd, Pt(2), $^1J_{Pt(2),P(3)} = 3626$ Hz, $^1J_{Pt(2),P(4)} = 2421$ Hz, $^1J_{Pt(2),P(2)} = 1291$ Hz, $^2J_{Pt(2),P(1)} = 295$ Hz) ppm.

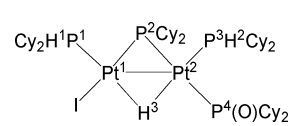

Syn-[(PHCy$_2$)(I)Pt(μ-PCy$_2$)(μ-H)Pt(PHCy$_2$){P(OH)Cy$_2$}]I (Pt−Pt) (9). An aqueous 0.5 M HI solution (0.35 mL) was added at room temperature under vigorous stirring to a dichloromethane solution of **1** (103 mg, 0.09 mmol in 5 mL) giving a pale yellow solution.

After 30 min, the time required for the $^{31}P\{^1H\}$ NMR to show the complete disappearance of **8**, the organic phase was separated, dried over Na_2SO_4, and filtered. The solvent was evaporated, and the crude was treated with toluene. The solid obtained after filtration was washed with toluene (3 × 4 mL) and *n*-hexane (3 × 4 mL) and dried with a gentle stream of dinitrogen. Yield about 40 mg (ca. 32%).

Complex **9** is unstable at room temperature both in the solid state and in solution because it transforms spontaneously into **7**. The transformation in the solid state is faster under reduced pressure thus hampering elemental and HR-MS analyses. The IR spectrum was recorded immediately after the isolation.

Complex **9** is soluble in halogenated solvents, insoluble in toluene and *n*-hexane.

IR (KBr, cm^{-1}): $\bar{\nu}$ = 3446 broad w (P−O−H), 2925 s, 2850 s, 2658 w, 2335 w (P−H), 1632 w (Pt−H−Pt), 1495 w, 1447 s, 1346 w, 1329 w, 1296 w, 1267 m, 1204 w, 1179 m, 1107 m, 1004 s, 917 s (P−O−H), 877 s, 848 m, 818 m, 800 w, 735 m, 530 w, 521 m, 471 m, 457 w, 413 w, 385 w.

^1H NMR (CD_2Cl_2, δ): 4.80 (m, H(1), $^1J_{H(1),P(1)}$ = 354 Hz, $^2J_{H(1),Pt(1)}$ = 136 Hz), 5.19 (m, H(2), $^1J_{H(2),P(3)}$ = 372 Hz), −5.52 (m, H(3), $^2J_{H(3),P(2)}$ = 13 Hz, $^2J_{H(3),P(1)}$ = 68 Hz, $^2J_{H(3),P(4)}$ = 15 Hz, $^2J_{H(3),P(3)}$ = 72 Hz, $^1J_{H(3),Pt(1)}$ = 379 Hz, $^1J_{H(3),Pt(2)}$ = 539 Hz), 7.58 (s, H(4)) ppm.

$^{31}P\{^1H\}$ NMR (CD_2Cl_2, δ): 169.0 (dd, P(2), $^1J_{P(2),Pt(1)}$ = 2470 Hz, $^1J_{P(2),Pt(2)}$ = 1582 Hz, $^2J_{P(2),P(4)}$ = 283 Hz, $^2J_{P(2),P(3)}$ = 11 Hz), 122.7 (dd, P(4), $^1J_{P(4),Pt(2)}$ = 2691 Hz, $^2J_{P(4),Pt(1)}$ = 40 Hz, $^2J_{P(4),P(2)}$ = 283 Hz, $^2J_{P(4),P(3)}$ = 21 Hz), 6.6 (d, P(1), $^1J_{P(1),Pt(1)}$ = 3918 Hz, $^2J_{P(1),Pt(2)}$ = 221 Hz, $^3J_{P(1),P(3)}$ = 49 Hz), 1.9 (broad, P(3), $^2J_{P(3),Pt(2)}$ = 3464 Hz, $^2J_{P(3),Pt(1)}$ = 180 Hz, $^3J_{P(3),P(1)}$ = 49 Hz, $^2J_{P(3),P(4)}$ = 21 Hz, $^2J_{P(3),P(2)}$ = 11 Hz) ppm.

$^{195}Pt\{^1H\}$ NMR (CD_2Cl_2, δ): −5778 (dddd, Pt(1), $^1J_{Pt(1),P(1)}$ = 3918 Hz, $^1J_{Pt(1),P(2)}$ = 2470 Hz, $^2J_{Pt(1),P(3)}$ = 180 Hz, $^2J_{Pt(1),P(4)}$ = 40 Hz, $^1J_{Pt(1),Pt(2)}$ = 721 Hz), −5668 (dddd, Pt(2), $^1J_{Pt(2),P(3)}$ = 3464 Hz, $^1J_{Pt(2),P(4)}$ = 2691 Hz, $^1J_{Pt(2),P(2)}$ = 1582 Hz, $^2J_{Pt(2),P(1)}$ = 221 Hz, $^1J_{Pt(2),Pt(1)}$ = 721 Hz) ppm.

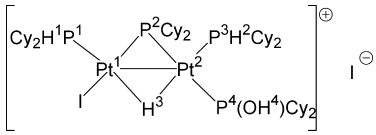

X-ray Crystallography[75]. Crystal data, parameters for intensity data collection and convergence results for **3**·$3CH_2Cl_2$ and **4**·$3CH_2Cl_2$ are compiled in Table 5. Diffraction quality crystals were grown from CH_2Cl_2/*n*-hexane. Data were collected with Mo Kα radiation (graphite monochromator, λ = 0.71073 Å) on a Bruker D8 goniometer with SMART CCD area detector on crystals of approximate dimensions 0.14 × 0.02 × 0.02 mm (**3**·$3CH_2Cl_2$) and 0.14 × 0.33 × 0.40 mm (**4**·$3CH_2Cl_2$). Multiscan absorption corrections with SADABS[76] (for **3**·$3CH_2Cl_2$) and PLATON[39] (for **4**·$3CH_2Cl_2$) were applied before averaging symmetry equivalent data. The structures were solved by direct methods[77] and refined with full-matrix least-squares on F^2.[78] All non-hydrogen atoms were refined anisotropically. Hydrogen atoms (except for the bridging one) were introduced in their idealized positions [d(CH) = 0.98 Å, d(CH) = 0.98 Å, d(PH) = 1.32 Å)] and refined using a riding model. The bridging hydrogen was treated as riding on Pt1 in a calculated position (on the plane formed by Pt1, Pt2 and P2, at a distance of ca. 1.7 Å from the metal atoms).

Table 5. Crystal Data and Structural Refinement Details for **3**·$3CH_2Cl_2$ and **4**·$3CH_2Cl_2$

	3·$3CH_2Cl_2$	**4**·$3CH_2Cl_2$
empirical formula	$C_{51}H_{98}OCl_8P_4Pt_2$	$C_{51}H_{98}OBr_2Cl_6P_4Pt_2$
formula mass	1524.95	1613.75
temperature [K]	110(2)	110(2)
wavelength [Å]	0.71073	0.71073
crystal system	triclinic	triclinic
space group	$P\bar{1}$	$P\bar{1}$
a [Å]	14.019(10)	13.8510(18)
b [Å]	15.335(11)	15.2389(19)
c [Å]	16.746(12)	16.563(2)
α [°]	105.574(12)	104.614(2)
β [°]	91.827(13)	92.913(2)
γ [°]	107.446(12)	107.145(2)
V [Å^3]	3284(4)	3202.9(7)
Z	2	2
$D_{calcd.}$ [Mg m^{-3}]	1.542	1.673
absorption coeff. [mm^{-1}]	4.711	5.994
θ range for data coll. [deg]	2.01−26.00	1.28−26.00
total reflections	37106	55997
independent reflections	9073	9583
data/parameters	12890/586	12574/606
goodness-of-fit on F^2	1.050	1.027
R^a ($I > 2\sigma(I)$)	0.0546	0.0443
wR_2^b (all data)	0.1564	0.1145
largest diff. peak/hole [e· Å^{-3}]	2.37/−2.47	2.61/−2.25

^{a} $R = \sum||F_o| - |F_c||/\sum|F_o|$. ^{b} $wR_2 = [\sum w(F_o^2 - F_c^2)^2/\sum w(F_o^2)^2]^{1/2}$.

Supporting Information Available: $^1H-^{31}P$ HMQC spectrum of complex **3**, $^{31}P\{^1H\}$ NMR and $^1H-^{195}Pt$ HMQC spectra of complexes **4**, **5**, **6**, **7**, **8**, **9**, **17**, HR-MS spectrograms of complexes **3a**, **4**, **5**, **6**, **7**, **8**, **17** and a displacement ellipsoid plot of **4**. This material is available free of charge via the Internet at http://pubs.acs.org.

IC800508T

(75) Crystallographic data (excluding structure factors) for **3**·$3CH_2Cl_2$ and **4**·$3CH_2Cl_2$ have been deposited with the Cambridge Crystallographic Data Centre (CCDC) as supplementary publications no. CCDC 664298 (**3**·$3CH_2Cl_2$) and CCDC 664299 (**4**·$3CH_2Cl_2$). Copies of the data can be obtained free of charge on application to CCDC, 12 Union Road, Cambridge CB2 1EZ, U.K. [Fax: int. code +44(1223)336−033; E-mail: deposit@ccdc.cam.ac.uk].

(76) Sheldrick, G. M. *SADABS, Program for Empirical Absorption Correction of Area Detector Data*; University of Göttingen: Göttingen, Germany, 1996.

(77) Sheldrick, G. M. *SHELXS97, Program for Crystal Structure Solution*; University of Göttingen: Göttingen, Germany, 1997.

(78) Sheldrick, G. M. *SHELXL97, Program for Crystal Structure Refinement*; University of Göttingen: Göttingen, Germany, 1997.